

Connection between GW and Extended Coupled Cluster

Johannes Tölle,^{1, a)} Marios-Petros Kitsaras,^{2, b)} Andreas Irmller,^{3, c)} Andreas Grüneis,^{3, d)} and Pierre-François Loos^{2, e)}

¹⁾Department of Chemistry, University of Hamburg, 22761 Hamburg, Germany; The Hamburg Centre for Ultrafast Imaging (CUI), Hamburg 22761, Germany

²⁾Laboratoire de Chimie et Physique Quantiques (UMR 5626), Université de Toulouse, CNRS, Toulouse, France

³⁾Institute for Theoretical Physics, TU Wien, Wiedner Hauptstraße 8-10/136, Vienna, Austria

Coupled-cluster (CC) theory and Green's function many-body perturbation theory (MBPT) have long evolved as distinct yet complementary frameworks for describing electronic correlation. While CC methods employ exponential wavefunction parametrizations that guarantee size extensivity and systematic improvability, Green's function approaches such as the GW approximation describe quasiparticle and optical excitations through diagrammatic resummations. Recent analyses have established a formal correspondence between these frameworks: the GW approximation is equivalent to an equation-of-motion (EOM) treatment of the direct-ring coupled-cluster doubles (drCCD) method. Within this context, the extended CC (ECC) ansatz offers a unified framework connecting CC and MBPT. This formulation bridges CC-based and Green's function-based methods, providing novel avenues for incorporating vertex corrections within a CC framework that keep a positive semi-definite self-energy and lead to potentially systematically improvable Green's function approaches.

I. INTRODUCTION

Coupled-cluster (CC) theory is one of the most mature and powerful methodologies in electronic structure theory.^{1–5} Developed over several decades, it now provides access not only to highly accurate ground-state energetics and properties but also to excited states, through either the equation-of-motion (EOM) or linear-response formalisms.^{6–10} Thanks to the sustained efforts of many research groups, CC has become the reference method for high-accuracy electronic structure calculations in molecular systems.^{11–21}

Inspired by the seminal work of Hubbard,²² the CC ansatz was originally introduced by Coester and Kümmel in the 1950s to describe correlations in nuclear matter.^{23,24} It was then brought into quantum chemistry in the 1960s through the seminal work of Sinanoğlu, Čížek, Paldus, and Shavitt.^{25–27} Interestingly, the method later migrated back to nuclear physics in the 1990s²⁸ and is now widely used for accurate computations of atomic nuclei.^{29–31} More recently, CC has also found applications in condensed matter physics, where methodological and algorithmic advances have enabled its deployment in periodic solids.^{32–40}

Decades of development have revealed both the strengths and limitations of CC theory. On the one hand, CC excels at describing ground- and excited-state properties of weakly correlated systems. The CCSD(T) model, in particular, is widely regarded as the “gold standard” of quantum chemistry,^{41,42} with systematic extensions such as CCSDT(Q)⁴³ providing a “platinum standard” for even higher accuracy.⁴⁴ The introduction of the Lagrangian formalism by Helgaker and co-workers placed the computation of properties as analytic gradients on firm theoretical grounds, opening the way to accurate calculations

of both static and frequency-dependent molecular properties of arbitrary order.^{45–51}

On the other hand, the single-reference nature of traditional CC theory becomes problematic in multireference situations where the Hartree–Fock (HF) determinant is not a suitable starting point. In such cases, higher-rank excitations (triples, quadruples, etc.) are often required, an EOM-CC approach may be employed,^{52–56} or one must turn to one of the various flavors of multireference CC.^{57–62}

A parallel story can be told for Green's function many-body perturbation theory (MBPT).^{63,64} Inspired by nuclear physics, with early contributions from Salpeter and Bethe,⁶⁵ Green's function approaches became central in condensed matter physics in the 1960s. Hedin's introduction of the GW approximation^{66–68} was a decisive turning point, as the concept of electronic screening proved remarkably successful in the description of the uniform electron gas.^{69–71} However, GW was not applied to realistic materials until the 1980s.^{72–77} While Green's function techniques such as the algebraic diagrammatic construction (ADC)^{78,79} were already being developed for molecules in the 1970s by Cederbaum, Schirmer, von Niessen, Domcke, and coworkers,^{80–87} the transfer of the GW and Bethe–Salpeter equation (BSE) formalism to quantum chemistry occurred only more recently.^{88–96} This was partly because screening effects were thought to be less dominant in small- and medium-sized molecular systems. Today, however, both GW ^{97,98} and BSE^{99,100} are widely used in molecular science, complementing traditional wavefunction approaches.

In recent years, several groups have begun to explore the theoretical connections between CC theory and Green's function MBPT. For example, Lange and Berkelbach analyzed the diagrammatic content of GW and ionization potential (IP) and electron affinity (EA) EOM-CC theory,^{8,52,53,101–103} identifying both striking similarities and key differences between the two.¹⁰⁴ They showed that EOM-CC with singles and doubles (EOM-CCSD)^{7,8,41,47,105,106} contains fewer ring diagrams than GW , but incorporates a large number of vertex corrections (i.e., beyond ring diagrams) arising from ladder, mixed ring-ladder, and exchange diagrams. Including triples yields EOM-

^{a)}Electronic mail: johannes.tolle@uni-hamburg.de

^{b)}Electronic mail: kitsaras@irsamc.ups-tlse.fr

^{c)}Electronic mail: andreas.irmller@tuwien.ac.at

^{d)}Electronic mail: andreas.grueneis@tuwien.ac.at

^{e)}Electronic mail: loos@irsamc.ups-tlse.fr

CCSDT,^{101,107–111} which includes all diagrams contained in the *GW* approximation, along with many additional high-order vertex corrections. Their work builds on earlier insights by Scuseria and co-workers,^{112,113} who related diagrammatic truncations of CC with doubles (CCD) to variants of the random-phase approximation (RPA) (see also Refs. 114–118).

More recently, Quintero-Monsebaiz *et al.* established connections between BSE@*GW* and CC at both the ground- and excited-state levels, enabling transfer of methodological insights from one framework to the other.¹¹⁹ They further showed that both *GW* and BSE can be recast as nonlinear CC-like equations solvable with the standard CC machinery with the same computational scaling. In the same spirit, Coveney and Tew have investigated the interconnections between various MBPT schemes and CCD, with a particular focus on the CC self-energy and Green's function.^{120–122} Building on the “upfolded” version of *GW* introduced by Bintrim and Berkelbach,¹²³ Tölle and Chan subsequently uncovered an exact connection between *GW* and the unitary CCD ansatz restricted to the direct-ring (dr) diagrams (drCCD).¹²⁴ These developments have already borne fruit: One of the authors of the present study derived the first fully analytic *GW* nuclear gradients,¹²⁵ and this work was recently extended by some of us to the first analytic BSE nuclear gradients.¹²⁶ Nevertheless, this strategy requires the numerical evaluation of an infinite series of nested (anti)commutators, which is not standard in conventional CC implementations. Unfortunately, direct application of EOM-CCD to *GW* remains hampered by missing correlation effects, as analyzed in Refs. 117 and 124. Very recently, some of us introduced a reformulation of the *GW* formalism that builds upon the well-established EOM-drCCD framework,¹²⁷ providing an alternative, fully analytic route to *GW* nuclear gradients. This modified EOM-CCD formulation restores the missing correlation effects inherent to traditional CCD-based approaches while maintaining a consistent and rigorous connection with the *GW* approximation.

In this context, the extended CC (ECC) ansatz of Arponen offers a promising path forward.¹²⁸ ECC generalizes standard CC by introducing a bi-variational framework,^{128–131} in which both excitation and de-excitation operators are optimized simultaneously (see also Ref. 132–134). This ansatz preserves size-extensivity while providing a (bi)variational energy functional, making it particularly well-suited for the evaluation of molecular properties. In particular, the bi-variational structure ensures that the Hellmann–Feynman theorem can be directly applied, thereby simplifying the computation of response properties.^{135–139}

Closely related to the ECC framework is the XCC approach,^{140,141} for which a straightforward EOM variant can be formulated.¹³² Both ECC and XCC employ a doubly similarity-transformed Hamiltonian, which introduces further low-lying correlation contributions, such as important third-order perturbation theory terms that are absent in conventional EOM-CCSD.^{104,132}

Comparative benchmark studies of various CC ansätze, including ECC, have been performed by Cooper and Knowles,¹⁴² as well as Evangelista.¹⁴³ Van Voorhis and Head-Gordon introduced the quadratic CCD method via a simplification of the

ECCD equations to preserve the computational scaling of the traditional CCD.¹⁴⁴ In the present contribution, we revisit the relationship between *GW* and ECC and demonstrate how the latter can provide a natural framework for embedding Green's function formalisms within the CC machinery.

The present work is organized as follows. Sections II and III introduce the *GW* approximation using two complementary frameworks: Hedin's approach and the electron-boson formulation, respectively. Section IV briefly reviews the traditional CC energy functional and the extended CC approach, which employs a double similarity transformation that plays a central role in this work. Section V applies an ECC-like double similarity transformation to the electron-boson Hamiltonian for the *GW* approximation introduced in Sec. III. This yields an ECC electron-boson Hamiltonian, which is represented in Fock space in Sec. VI, yielding an eigenvalue problem for charged excitation energies. Section VII demonstrates the equivalence between the eigenvalue problem of the ECC electron-boson Hamiltonian (Sec. VI) and the *GW* supermatrix (Sec. III). Section VIII identifies the terms in the ECC electron-boson formulation that correspond to vertex corrections beyond *GW*. In Sec. IX, we motivate a low-order approximation to the *GW* density matrix within the framework of the double similarity transformed Hamiltonian. The resulting linearized one-body density matrix yields an additional correction in the Fock matrix, which can be viewed as an approximation to self-consistent *GW*. Computational details are summarized in Sec. X. Numerical results for principal and secondary IPs of a molecular test set are reported in Sec. XI, where different levels of theory and vertex corrections are compared. Finally, conclusions are drawn in Sec. XII.

II. THE *GW* APPROXIMATION

The *GW* approximation is most rigorously formulated within the framework of Hedin's equations,⁶⁶ which constitute a self-consistent set of five coupled integro-differential relations connecting the one-body Green's function G , the dynamically screened Coulomb interaction W , the irreducible vertex function Γ , the irreducible polarizability P , and the exchange-correlation (xc) self-energy Σ_{xc} :

$$\Gamma(123) = \delta(12)\delta(13) + \frac{\delta\Sigma_{\text{xc}}(12)}{\delta G(45)}G(46)G(75)\Gamma(673) \quad (1a)$$

$$P(12) = -iG(13)G(41)\Gamma(342) \quad (1b)$$

$$W(12) = v(12) + v(13)P(34)W(42) \quad (1c)$$

$$\Sigma_{\text{xc}}(12) = iG(14)W(1^+3)\Gamma(423) \quad (1d)$$

$$G(12) = G_{\text{H}}(12) + G_{\text{H}}(13)\Sigma_{\text{xc}}(34)G(42) \quad (1e)$$

where v denotes the bare Coulomb interaction, and G_{H} is the Hartree (H) Green's function. Here, integer numbers denote combined space-spin-time variables.

The *GW* approximation arises upon replacing the three-point irreducible vertex Γ by its zeroth-order form, $\Gamma(123) = \delta(12)\delta(13)$, which neglects vertex corrections beyond the independent-particle response. Under this approximation, the

irreducible polarizability reduces to

$$P(12) = -iG(12)G(21) \quad (2)$$

and the xc self-energy simplifies to

$$\Sigma_{xc}(12) = iG(12)W(1^+2) \quad (3)$$

Systematic improvements beyond GW can then be obtained by including vertex corrections in either P (internal corrections) or Σ_{xc} (external corrections).^{145–162}

It is worth noting that both G and W satisfy Dyson-like equations [see Eqs. (1c) and (1d), respectively], with Σ_{xc} and P serving as their respective kernels. This observation highlights that the GW approximation is inherently a two-step procedure. In the first step, P is computed to determine the dynamical screening W . In the second step, Σ_{xc} is evaluated in order to obtain the one-body Green's function G .

An alternative and particularly transparent way to view the GW approximation is through its supermatrix representation.^{119,123,163–167} In this formalism, GW can be written as a linear eigenvalue problem of the form

$$\mathbf{H}^{GW} \cdot \mathbf{R} = \mathbf{R} \cdot \mathbf{E} \quad (4)$$

where \mathbf{E} gathers the charged excitation energies (quasiparticle and satellites), the GW supermatrix reads

$$\mathbf{H}^{GW} = \begin{pmatrix} \mathbf{f} & \mathbf{M}^{2h1p} & \mathbf{M}^{2p1h} \\ (\mathbf{M}^{2h1p})^\dagger & \mathbf{C}^{2h1p} & \mathbf{0} \\ (\mathbf{M}^{2p1h})^\dagger & \mathbf{0} & \mathbf{C}^{2p1h} \end{pmatrix} \quad (5)$$

and

$$\mathbf{R} = \begin{pmatrix} \mathbf{r} \\ \mathbf{r}^{2h1p} \\ \mathbf{r}^{2p1h} \end{pmatrix} \quad (6)$$

Here, \mathbf{f} is the Fock matrix containing the one-hole (1h) and one-particle (1p) configurations, and diagonal sub-blocks defined as

$$C_{iv,iv}^{2h1p} = \epsilon_i - \Omega_v \quad C_{av,av}^{2p1h} = \epsilon_a + \Omega_v \quad (7)$$

for the two-hole-one-particle (2h1p) and two-particle-one-hole (2p1h) configurations, where ϵ_p are the quasiparticle energies. The corresponding coupling matrices,

$$M_{pi,iv}^{2h1p} = M_{pi,v} \quad M_{pa,av}^{2p1h} = M_{pa,v} \quad (8)$$

contain the effective two-electron integrals,

$$M_{pq,v} = \sum_{ia} \langle pa|qi \rangle (X + Y)_{ia,v} \quad (9)$$

where \mathbf{X} and \mathbf{Y} are the RPA excitation and deexcitation vectors associated with the one-hole-one-particle (1h1p) RPA (positive) excitation energies Ω_v (see below). The two-electron integrals $\langle pq|rs \rangle$ are given in Dirac notation, i.e., $\langle 12|12 \rangle$. In this work, the indices p, q, r, s, \dots are used for arbitrary orbitals, i, j, k, l label the occupied orbitals, a, b, c, d denote the

virtual orbitals, and μ, ν, \dots (collective) combined particle-hole indices. Furthermore, real-valued orbitals are assumed throughout.

The above linear eigenvalue problem can equivalently be recast as a nonlinear quasiparticle equation,

$$[\mathbf{f} + \Sigma_c(\omega) - \omega \mathbf{1}] \cdot \mathbf{r} = \mathbf{0} \quad (10)$$

where the correlation self-energy takes the form

$$\Sigma_c(\omega) = \mathbf{M}^{2h1p} \cdot (\omega \mathbf{1} - \mathbf{C}^{2h1p})^{-1} \cdot (\mathbf{M}^{2h1p})^\dagger + \mathbf{M}^{2p1h} \cdot (\omega \mathbf{1} - \mathbf{C}^{2p1h})^{-1} \cdot (\mathbf{M}^{2p1h})^\dagger \quad (11)$$

The elements of the correlation part of the self-energy read

$$(\Sigma_c)_{pq}(\omega) = \sum_{iv} \frac{M_{pi,v} M_{qi,v}}{\omega - \epsilon_i + \Omega_v} + \sum_{av} \frac{M_{pa,v} M_{qa,v}}{\omega - \epsilon_a - \Omega_v} \quad (12)$$

The matrices \mathbf{X} and \mathbf{Y} are obtained by solving the direct RPA eigenvalue problem,

$$\begin{pmatrix} \mathbf{A} & \mathbf{B} \\ -\mathbf{B} & -\mathbf{A} \end{pmatrix} \cdot \begin{pmatrix} \mathbf{X} & \mathbf{Y} \\ \mathbf{Y} & \mathbf{X} \end{pmatrix} = \begin{pmatrix} \mathbf{X} & \mathbf{Y} \\ \mathbf{Y} & \mathbf{X} \end{pmatrix} \cdot \begin{pmatrix} \mathbf{\Omega} & \mathbf{0} \\ \mathbf{0} & -\mathbf{\Omega} \end{pmatrix} \quad (13)$$

where

$$A_{ia,jb} = (\epsilon_a - \epsilon_i) \delta_{ij} \delta_{ab} + \langle ib|aj \rangle \quad (14a)$$

$$B_{ia,jb} = \langle ij|ab \rangle \quad (14b)$$

Solving this RPA problem, which scales as $O(N^6)$, is a prerequisite for constructing the GW supermatrix. It can be shown to be equivalent to solving the Riccati equation¹¹²

$$\mathbf{B} + \mathbf{A} \cdot \mathbf{t} + \mathbf{t} \cdot \mathbf{A} + \mathbf{t} \cdot \mathbf{B} \cdot \mathbf{t} = \mathbf{0} \quad (15)$$

with

$$\mathbf{t} = \mathbf{Y} \cdot \mathbf{X}^{-1} \quad (16)$$

Although this formal equivalence is useful, it does not by itself provide a clear physical interpretation of the GW approximation. Nevertheless, it clearly shows that introducing vertex corrections within the same excitation manifold (i.e., up to 2h1p and 2p1h configurations) can only be achieved by modifying one or more of the following quantities in Eq. (5): the Fock matrix \mathbf{f} , the diagonal blocks \mathbf{C} , or the coupling blocks \mathbf{M} .

III. GW AS A ELECTRON-BOSON PROBLEM

A complementary and highly insightful perspective on the GW approximation is obtained by recasting it as an electron-boson coupling model.^{165,168–171} Within this picture, an electron added to or removed from the system interacts linearly with a bath of bosonic excitations representing the collective electronic response.¹⁶⁵ In this framework, the RPA excitations are interpreted as effective bosonic modes that mediate the

dynamical screening of the Coulomb interaction. The resulting Hamiltonian reads

$$\hat{H}_{\text{eB}} = \hat{H}_{\text{e}} + \hat{H}_{\text{B}} + \hat{V}_{\text{eB}} \quad (17)$$

where

$$\hat{H}_{\text{e}} = \sum_{pq} f_{pq} \hat{a}_p^\dagger \hat{a}_q \quad (18a)$$

$$\hat{H}_{\text{B}} = \sum_{\mu\nu} A_{\mu\nu} \hat{b}_\mu^\dagger \hat{b}_\nu + \frac{1}{2} \sum_{\mu\nu} B_{\mu\nu} (\hat{b}_\mu^\dagger \hat{b}_\nu^\dagger + \hat{b}_\mu \hat{b}_\nu) \quad (18b)$$

$$\hat{V}_{\text{eB}} = \sum_{pq\nu} V_{pq,\nu} \hat{a}_p^\dagger \hat{a}_q (\hat{b}_\nu^\dagger + \hat{b}_\nu) \quad (18c)$$

respectively describe the fermionic subsystem, the bosonic bath, and their mutual coupling. Here, f_{pq} is an element of the Fock matrix, $V_{pq,\nu} \equiv V_{pq,ia} = \langle pa|qi \rangle$ are two-electron integrals that mediate the coupling between the electronic and bosonic degrees of freedom, and the elements of the particle-conserving and particle-non-conserving components of the bosonic Hamiltonian are given by [see Eq. (14)]

$$A_{\mu\nu} \equiv A_{ia,jb} \quad B_{\mu\nu} \equiv B_{ia,jb} \quad (19)$$

Although neutral electronic excitations are fundamentally composed of fermions, they can often be treated approximately as bosons. In this framework, quasiboson creation and annihilation operators emulate fermionic particle-hole excitations,

$$\hat{b}_\nu^\dagger = \hat{a}_a^\dagger \hat{a}_i \quad \hat{b}_\nu = \hat{a}_i^\dagger \hat{a}_a \quad (20)$$

where \hat{a}_a^\dagger and \hat{a}_i denote fermionic creation and annihilation operators, respectively. Because of their underlying fermionic structure, these quasiboson operators do not strictly satisfy fermionic anti-commutation relations anymore, and therefore violate the Pauli exclusion principle and the antisymmetry of the exact electronic wavefunction.¹¹² The quasiboson approximation consists in neglecting these deviations and treating quasibosons as ideal bosons. This approximation not only simplifies the algebra and the physical interpretation of excitation processes but also transforms otherwise *quartic* fermionic operators, such as the two-body part of the electronic Hamiltonian, into effective (bosonized) *quadratic* Hamiltonians in the quasiboson operators.

Using the composite basis made of the union of the 1h $\{\hat{a}_i\}$, 1p $\{\hat{a}_a\}$, 2h1p $\{\hat{a}_i \hat{b}_\nu^\dagger\}$, and 2p1h $\{\hat{a}_a \hat{b}_\nu\}$ configurations, an IP/EAO-EOM treatment on the electron-boson Hamiltonian naturally yields the *GW* supermatrix within the Tamm-Dancoff approximation (TDA).¹²³

To go beyond the TDA, the bosonic Hamiltonian must be diagonalized through a Bogoliubov transformation, which is conveniently expressed as¹⁶⁵

$$\hat{H}_{\text{B}} = -\frac{1}{2} \text{Tr } A + \frac{1}{2} (\mathbf{b}^\dagger \quad \mathbf{b}) \cdot \begin{pmatrix} \mathbf{A} & \mathbf{B} \\ \mathbf{B} & \mathbf{A} \end{pmatrix} \cdot (\mathbf{b}^\dagger) \quad (21)$$

Introducing the quasiparticle (Bogoliubov) operators¹⁷²

$$\begin{pmatrix} \boldsymbol{\beta} \\ \boldsymbol{\beta}^\dagger \end{pmatrix} = \begin{pmatrix} \mathbf{X} & -\mathbf{Y} \\ -\mathbf{Y} & \mathbf{X} \end{pmatrix}^\dagger \cdot \begin{pmatrix} \mathbf{b} \\ \mathbf{b}^\dagger \end{pmatrix} \quad (22)$$

defined through a unitary transformation built from the RPA eigenvectors, the Hamiltonian becomes

$$\hat{H}_{\text{B}} = -\frac{1}{2} \text{Tr } A + \frac{1}{2} (\boldsymbol{\beta}^\dagger \quad \boldsymbol{\beta}) \cdot \begin{pmatrix} \boldsymbol{\Omega} & \mathbf{0} \\ \mathbf{0} & \boldsymbol{\Omega} \end{pmatrix} \cdot \begin{pmatrix} \boldsymbol{\beta} \\ \boldsymbol{\beta}^\dagger \end{pmatrix}. \quad (23)$$

The components of the Hamiltonian can then be recast as

$$\hat{H}_{\text{B}} = E_{\text{c}} + \sum_{\mu} \Omega_{\mu} \hat{b}_{\mu}^\dagger \hat{b}_{\mu} \quad (24a)$$

$$\hat{V}_{\text{eB}} = \sum_{\mu\nu} M_{\mu\nu} \hat{a}_\mu^\dagger \hat{a}_\nu (\hat{b}_\nu^\dagger + \hat{b}_\nu) \quad (24b)$$

where the RPA correlation energy is

$$E_{\text{c}} = \frac{1}{2} \text{Tr}(\boldsymbol{\Omega} - A) \quad (25)$$

The particle-nonconserving bosonic terms in \hat{H}_{B} are thus removed by the Bogoliubov transformation that diagonalizes the RPA problem. However, full diagonalization is not strictly necessary: a block-diagonalization already suffices to decouple excitation and deexcitation subspaces, rendering the unitary Bogoliubov transformation somewhat excessive. In the following sections, we will first introduce the extended CC approach and then show that an equivalent block-diagonal structure can be achieved more directly through a double similarity transformation.

IV. EXTENDED COUPLED CLUSTER

The traditional CC (TCC) energy functional is

$$E_{\text{TCC}} = \langle \Phi_0 | (1 + \hat{\Lambda}) e^{-\hat{T}} \hat{H} e^{\hat{T}} | \Phi_0 \rangle \quad (26)$$

where $\hat{T} = \sum_q t_q \hat{\tau}_q$ is an excitation operator written as a function of the general excitation operator $\hat{\tau}_q$ and $\hat{\Lambda} = \sum_q \lambda_q \hat{\tau}_q^\dagger$ is a deexcitation operator. These operators act on the reference wave function Φ_0 to generate excited determinant Φ_q as $|\Phi_q\rangle = \hat{\tau}_q |\Phi_0\rangle$ and $\langle \Phi_q | = \langle \Phi_0 | \hat{\tau}_q^\dagger$.

The extended CC energy bi-functional is

$$E_{\text{ECC}} = \langle \Phi_0 | e^{\hat{Z}} e^{-\hat{T}} \hat{H} e^{\hat{T}} e^{-\hat{Z}} | \Phi_0 \rangle \quad (27)$$

where the linear operator $1 + \hat{\Lambda}$ has been replaced by a proper exponential operator $e^{\hat{Z}}$ with $\hat{Z} = \sum_q z_q \hat{\tau}_q^\dagger$. In other words, TCC can be seen as an approximation of ECC. Making the ECC energy functional stationary with respect to the right amplitudes t_q and left amplitudes z_q , i.e.,

$$\frac{\partial E_{\text{ECC}}}{\partial z_q} = 0 \quad \frac{\partial E_{\text{ECC}}}{\partial t_q} = 0 \quad (28)$$

yields the amplitude equations

$$\langle \Phi_q | e^{\hat{Z}} e^{-\hat{T}} \hat{H} e^{\hat{T}} | \Phi_0 \rangle = 0 \quad (29a)$$

$$\langle \Phi_0 | e^{\hat{Z}} e^{-\hat{T}} [\hat{H}, \hat{\tau}_q] e^{\hat{T}} | \Phi_0 \rangle = 0 \quad (29b)$$

which, contrary to TCC, couple the two sets of amplitudes. Note that an alternative formulation of the ECC amplitude equations through projection exists,¹³² and numerical results for ground-state energies using both schemes have been shown to be similar.^{133,134}

When restricted to double excitations, that is, $\hat{T} = \hat{T}_2$, the ECC energy functional becomes

$$\begin{aligned} E_{\text{ECC}} &= \langle \Phi_0 | e^{\hat{Z}} (\hat{H} e^{\hat{T}_2})_c | \Phi_0 \rangle \\ &= \langle \Phi_0 | e^{\hat{Z}} \left(\hat{H} + \hat{H}\hat{T}_2 + \frac{1}{2}\hat{H}\hat{T}_2^2 + \frac{1}{6}\hat{H}\hat{T}_2^3 + \frac{1}{24}\hat{H}\hat{T}_2^4 \right)_c | \Phi_0 \rangle \\ &= \langle \Phi_0 | \hat{H} + \hat{Z} \left(\hat{H} + \hat{H}\hat{T}_2 + \frac{1}{2}\hat{H}\hat{T}_2^2 \right)_c \\ &\quad + \frac{1}{2}\hat{Z}^2 \left(\frac{1}{2}\hat{H}\hat{T}_2^2 + \frac{1}{6}\hat{H}\hat{T}_2^3 \right)_c + \frac{1}{6}\hat{Z}^3 \left(\frac{1}{24}\hat{H}\hat{T}_2^4 \right)_c | \Phi_0 \rangle \end{aligned} \quad (30)$$

The subscript c stands for “connected” and replaces (nested) commutator(s) between the Hamiltonian and the cluster operator, e.g., $[\hat{H}, \hat{T}_2] = (\hat{H}\hat{T}_2)_c$, as only connected terms survive in these contributions.

At this stage, it is useful to emphasize the similarities and differences between the unitary and extended CC ansätze. The ECC form, $e^{\hat{Z}} e^{-\hat{T}} \hat{H} e^{\hat{T}} e^{-\hat{Z}}$, can be recast as $e^{-\hat{T}} \hat{H} e^{\hat{T}}$ by defining $\hat{t} = \hat{T} - \hat{Z} + \frac{1}{2}[\hat{Z}, \hat{T}] + \dots$, sharing some resemblance with the unitary CC (UCC) expression with $\hat{t} = \hat{T} - \hat{T}^\dagger$. In UCC, the anti-Hermiticity condition $\hat{t}^\dagger = -\hat{t}$ ensures a unitary transformation. In contrast, ECC does not enforce this constraint: \hat{Z} is independent of \hat{T} , making \hat{t} generally non-Hermitian, offering greater flexibility at the cost of Hermiticity. Unlike the UCC functional, which results in a non-terminating Baker–Campbell–Hausdorff (BCH) expansion, the ECC approach results in a terminating series, although at a much higher order than the traditional CCD functional. Lastly, we mention the XCC parametrization that bears the same truncating doubly-similarity transformed Hamiltonian form as ECC but restricts the deexcitations to be the complex conjugate of the excitations $\hat{Z} = \hat{T}^\dagger$.¹³² It is argued that due to the decreased flexibility of the XCC ansatz, ECC is expected to recover Hermiticity more effectively in comparison.¹³²

The computational cost of traditional CCD is $O(N^6)$, whereas ECCD scales as $O(N^{10})$, which largely explains why it has not been widely adopted despite its attractive formal properties. Henderson and Scuseria demonstrated that the pair-ECCD method achieves the same $O(N^3)$ scaling as the corresponding pair-CCD approach.^{173,174} Likewise, van Voorhis and Head-Gordon showed that truncating $e^{\hat{Z}}$ after the quadratic term reduces the scaling to $O(N^6)$.¹⁴⁴ These results suggest that suitable restrictions on the double excitation operator can significantly lower the computational cost of ECCD. Below, we will show that the quadratic nature of the bosonic Hamiltonian underlying *GW* results in a significant simplification of both the working equations and the associated computational cost.

V. ECC ON THE ELECTRON-BOSON HAMILTONIAN

In this section, we apply the ECC ansatz to the bosonic Hamiltonian \hat{H}_B defined in Eq. (18b). As outlined in Sec. IV, a double similarity transformation is performed:

$$\bar{H}_B = e^{\hat{Z}} \bar{H}_B e^{-\hat{Z}} = e^{\hat{Z}} e^{-\hat{T}} \hat{H}_B e^{\hat{T}} e^{-\hat{Z}} \quad (31)$$

where the bosonic excitation and de-excitation operators are defined as

$$\hat{T} = \frac{1}{2} \sum_{\mu\nu} t_{\mu\nu} \hat{b}_\mu^\dagger \hat{b}_\nu^\dagger \quad \hat{Z} = \frac{1}{2} \sum_{\mu\nu} z_{\mu\nu} \hat{b}_\mu \hat{b}_\nu \quad (32)$$

Because \hat{H}_B is quadratic, the BCH expansion associated with the first similarity transformation truncates exactly at second order, yielding

$$\begin{aligned} \bar{H}_B &= \hat{H}_B + [\hat{H}_B, \hat{T}] + \frac{1}{2}[[\hat{H}_B, \hat{T}], \hat{T}] \\ &= \frac{1}{2} \sum_{\lambda\sigma} B_{\lambda\sigma} t_{\lambda\sigma} + \sum_{\mu\nu} \bar{A}_{\mu\nu} \hat{b}_\mu^\dagger \hat{b}_\nu \\ &\quad + \frac{1}{2} \sum_{\mu\nu} \bar{B}_{\mu\nu} \hat{b}_\mu^\dagger \hat{b}_\nu^\dagger + \frac{1}{2} \sum_{\mu\nu} B_{\mu\nu} \hat{b}_\mu \hat{b}_\nu \end{aligned} \quad (33)$$

with

$$\bar{A}_{\mu\nu} = A_{\mu\nu} + \sum_\lambda t_{\nu\lambda} B_{\lambda\mu} \quad (34a)$$

$$\bar{B}_{\mu\nu} = B_{\mu\nu} + \sum_\lambda A_{\mu\lambda} t_{\lambda\nu} + \sum_\lambda t_{\mu\lambda} A_{\lambda\nu} + \sum_{\lambda\sigma} t_{\mu\lambda} B_{\lambda\sigma} t_{\sigma\nu} \quad (34b)$$

where we made use of the fact that $t^T = t$.¹¹² As seen in Eq. (33), \bar{H}_B remains quadratic, containing both number-conserving and non-number-conserving terms. Hence, the second BCH expansion also terminates at second order, leading to

$$\begin{aligned} \bar{\bar{H}}_B &= \bar{H}_B + [\bar{Z}, \bar{H}_B] + \frac{1}{2}[\bar{Z}, [\bar{Z}, \bar{H}_B]] \\ &= \frac{1}{2} \sum_{\lambda\sigma} \bar{B}_{\lambda\sigma} z_{\lambda\sigma} + \sum_{\mu\nu} \bar{\bar{A}}_{\mu\nu} \hat{b}_\mu^\dagger \hat{b}_\nu \\ &\quad + \frac{1}{2} \sum_{\mu\nu} \bar{\bar{B}}_{\mu\nu} \hat{b}_\mu^\dagger \hat{b}_\nu^\dagger + \frac{1}{2} \sum_{\mu\nu} \bar{\bar{B}}_{\mu\nu} \hat{b}_\mu \hat{b}_\nu \end{aligned} \quad (35)$$

where

$$\bar{\bar{A}}_{\mu\nu} = \bar{A}_{\mu\nu} + \sum_\lambda z_{\nu\lambda} \bar{B}_{\lambda\mu} \quad (36a)$$

$$\bar{\bar{B}}_{\mu\nu} = B_{\mu\nu} + \sum_\lambda \bar{A}_{\mu\lambda} z_{\lambda\nu} + \sum_\lambda z_{\mu\lambda} \bar{A}_{\lambda\nu} + \sum_{\lambda\sigma} z_{\mu\lambda} \bar{B}_{\lambda\sigma} z_{\sigma\nu} \quad (36b)$$

Let $|0_B\rangle$ denote the bosonic reference vacuum. The right amplitude equations, obtained as $\langle 0_B | \hat{b}_\mu \hat{b}_\nu \bar{\bar{H}}_B | 0_B \rangle = 0$, yield the condition $\bar{\bar{B}}_{\mu\nu} = 0$, which is equivalent to the (quadratic) Riccati equation in Eq. (15). The left amplitude equations,

$\langle 0_B | \bar{H}_B \hat{b}_\mu^\dagger \hat{b}_\nu^\dagger | 0_B \rangle = 0$, give $\bar{B}_{\mu\nu} = 0$, which reduces to a set of linear equations in $z_{\mu\nu}$ once $\bar{B}_{\mu\nu} = 0$:

$$\bar{B}_{\mu\nu} + \sum_\lambda \bar{A}_{\mu\lambda} z_{\lambda\nu} + \sum_\lambda z_{\mu\lambda} \bar{A}_{\lambda\nu} = 0 \quad (37)$$

Note that, although left- and right-amplitude equations are generally coupled, they are completely decoupled in the present case.

Once these two conditions are satisfied, the double similarity-transformed bosonic Hamiltonian simplifies to

$$\bar{H}_B = \sum_{\mu\nu} \bar{A}_{\mu\nu} \hat{b}_\nu^\dagger \hat{b}_\mu + \frac{1}{2} \sum_{\lambda\sigma} B_{\lambda\sigma} t_{\lambda\sigma} \quad (38)$$

where all non-number-conserving terms have been eliminated.

Having established the ECC treatment of the bosonic Hamiltonian, we can now turn to the full electron-boson Hamiltonian \bar{H}_{eB} given in Eq. (17). The double similarity-transformed electron-boson Hamiltonian reads

$$\begin{aligned} \bar{H}_{eB} &= e^{\hat{Z}} e^{-\hat{T}} \hat{H}_{eB} e^{\hat{T}} e^{-\hat{Z}} \\ &= \bar{H}_{eB} + [\hat{Z}, \bar{H}_{eB}] \\ &= \hat{H}_e + \bar{H}_B + \bar{V}_{eB} \end{aligned} \quad (39)$$

with

$$\begin{aligned} \bar{V}_{eB} &= \sum_{pq} \sum_\nu V_{pq,\nu} \hat{a}_p^\dagger \hat{a}_q (\hat{b}_\nu^\dagger + \hat{b}_\nu) \\ &+ \sum_{pq} \sum_\nu \sum_\lambda V_{pq,\lambda} t_{\lambda\nu} \hat{a}_p^\dagger \hat{a}_q \hat{b}_\nu^\dagger \\ &+ \sum_{pq} \sum_\nu \left[\sum_\lambda V_{pq,\lambda} z_{\lambda\nu} + \sum_{\mu\lambda} V_{pq,\lambda} t_{\lambda\mu} z_{\mu\nu} \right] \hat{a}_p^\dagger \hat{a}_q \hat{b}_\nu \end{aligned} \quad (40)$$

VI. EOM ON THE ECC ELECTRON-BOSON HAMILTONIAN

Building on the ECC electron-boson Hamiltonian introduced in Sec. V, we next derive the EOM formulation for charged excitations. Within the present ECC-based formalism, the excitation operator $\bar{R}^{(m)}$ for the m th excited state is defined as

$$\begin{aligned} \bar{R}^{(m)} &= e^{\hat{T}} e^{-\hat{Z}} \hat{R}^{(m)} e^{\hat{Z}} e^{-\hat{T}} \\ &= \sum_M R_M^{(m)} \bar{c}_M = \sum_M R_M^{(m)} e^{\hat{T}} e^{-\hat{Z}} \hat{c}_M e^{\hat{Z}} e^{-\hat{T}} \\ &= \sum_i r_i^{(m)} a_i + \sum_{iv} r_{iv}^{(m)} \bar{b}_v^\dagger a_i + \sum_a r_a^{(m)} a_a + \sum_{av} r_{va}^{(m)} \bar{b}_v a_a \end{aligned} \quad (41)$$

where \hat{c}_M denotes an excitation operator associated with the M th excitation process [see Eq. (6)]. The various excitation channels are expressed in terms of double similarity-transformed bosonic creation and annihilation operators,

$$\bar{b}_\nu^\dagger = e^{\hat{T}} e^{-\hat{Z}} \hat{b}_\nu^\dagger e^{\hat{Z}} e^{-\hat{T}} \quad (42a)$$

$$\bar{b}_\nu = e^{\hat{T}} e^{-\hat{Z}} \hat{b}_\nu e^{\hat{Z}} e^{-\hat{T}} \quad (42b)$$

as well as the corresponding left and right reference states in the combined fermionic-bosonic space,

$$| 0_e \bar{0}_B \rangle = e^{\hat{T}} e^{-\hat{Z}} | 0_e 0_B \rangle \quad (43a)$$

$$\langle 0_e \bar{0}_B | = \langle 0_e 0_B | e^{\hat{Z}} e^{-\hat{T}} \quad (43b)$$

The use of these transformed creation and annihilation operators is essential to ensure that the EOM formalism satisfies the required “killer” conditions.^{175–180}

The EOM eigenvalue problem becomes

$$\langle 0_e \bar{0}_B | \left[\bar{c}_M^\dagger, [\bar{H}_{eB}, \bar{R}^{(m)}] \right] | 0_e \bar{0}_B \rangle = \langle 0_e \bar{0}_B | \left[\bar{c}_M^\dagger, \bar{R}^{(m)} \right] | 0_e \bar{0}_B \rangle E^{(m)} \quad (44)$$

with $E^{(m)}$ denoting the energy of the m th charged excited state, and \bar{c}_M^\dagger to the M th excitation/deexcitation process [see Eq. (41)], respectively. Equation (44) can be simplified to

$$\langle 0_e 0_B | \left[\bar{c}_M^\dagger, [\bar{H}_{eB}, \bar{R}^{(m)}] \right] | 0_e 0_B \rangle = \langle 0_e 0_B | \left[\hat{c}_M^\dagger, \hat{R}^{(m)} \right] | 0_e 0_B \rangle E^{(m)} \quad (45)$$

and the resulting EOM eigenvalue problem can be written as

$$\mathbf{H}^{\text{EOM}} \cdot \mathbf{R} = \mathbf{R} \cdot \mathbf{E} \quad (46)$$

The equivalence with the $G_0 W_0$ quasiparticle energies is established analytically in Sec. VII, identifying the matrix elements of the effective Hamiltonian \mathbf{H}^{EOM} with those of the GW supermatrix \mathbf{H}^{GW} defined in Eq. (5).

Details regarding the determination of analytic properties within the ECC treatment of the electron-boson Hamiltonian can be found in Ref. 127.

VII. EQUIVALENCE WITH $G_0 W_0$

Having derived the EOM quasiparticle equations using the ECC electron-boson Hamiltonian [see Eq. (46)], we now establish their analytical equivalence with the $G_0 W_0$ quasiparticle equations. For this, we rewrite the effective Hamiltonian \mathbf{H}^{EOM} in block form as

$$\mathbf{H}^{\text{EOM}} = \begin{pmatrix} \mathbf{f} & \tilde{\mathbf{N}}^{2\text{h1p}} & \mathbf{N}^{2\text{p1h}} \\ (\mathbf{N}^{2\text{h1p}})^\dagger & \mathbf{D}^{2\text{h1p}} & \mathbf{0} \\ (\tilde{\mathbf{N}}^{2\text{p1h}})^\dagger & \mathbf{0} & \mathbf{D}^{2\text{p1h}} \end{pmatrix} \quad (47)$$

The matrices read

$$[\tilde{\mathbf{N}}^{2\text{h1p}}]_{pi,\mu} = \sum_\nu V_{pi,\nu} \left(\delta_{\nu\mu} + z_{\nu\mu} + \sum_\lambda t_{\nu\lambda} z_{\lambda\mu} \right) \quad (48a)$$

$$[\tilde{\mathbf{N}}^{2\text{p1h}}]_{pa,\mu} = \sum_\nu V_{pa,\nu} \left(\delta_{\nu\mu} + z_{\nu\mu} + \sum_\lambda t_{\nu\lambda} z_{\lambda\mu} \right) \quad (48b)$$

$$[\mathbf{N}^{2\text{h1p}}]_{pi,\mu} = \sum_\nu V_{pi,\nu} (\delta_{\nu\mu} + t_{\nu\mu}) \quad (48c)$$

$$[\mathbf{N}^{2\text{p1h}}]_{pa,\mu} = \sum_\nu V_{pa,\nu} (\delta_{\nu\mu} + t_{\nu\mu}) \quad (48d)$$

and

$$[\mathbf{D}^{2\text{h1p}}]_{iv,j\mu} = f_{ij} - A_{\nu\mu} - \sum_\lambda t_{\nu\lambda} B_{\lambda\mu} \quad (49a)$$

$$[\mathbf{D}^{2\text{p1h}}]_{av,b\mu} = f_{ab} + A_{\nu\mu} + \sum_\lambda B_{\nu\lambda} t_{\lambda\mu} \quad (49b)$$

To demonstrate the equivalence of Eq. (46) with the G_0W_0 supermatrix [see Eq. (5)], we begin by establishing the following relation $(\mathbf{1} + \mathbf{t}) \cdot \mathbf{X} = \mathbf{X} + \mathbf{Y}$, which follows directly from Eq. (16). Furthermore, we note that $\mathbf{1} + \mathbf{z} + \mathbf{t} \cdot \mathbf{z} = (\mathbf{1} - \mathbf{t})^{-1}$ (see the [Supplementary Material](#)), simplifying Eqs. (48a)-(48b). From these relations, one finds that $(\mathbf{1} - \mathbf{t})^{-1} \cdot \mathbf{X}^{-1} = (\mathbf{X} - \mathbf{Y})^{-1} = \mathbf{X} + \mathbf{Y}$, where we made use of $\mathbf{t}^T = \mathbf{t}$.¹¹² Finally, one can show that¹²⁷

$$\mathbf{X} \cdot (\mathbf{A} + \mathbf{t} \cdot \mathbf{B}) \cdot \mathbf{X}^{-1} = \mathbf{\Omega} \quad (50)$$

Using the relations derived above, the EOM-ECC eigenvalue problem can be rewritten as

$$\mathbf{H}^{\text{EOM}} \cdot \mathbf{S}^{-1} \cdot \mathbf{S} \cdot \mathbf{R} = \mathbf{R} \cdot \mathbf{E} \quad (51)$$

which, after multiplication from the left by the metric

$$\mathbf{S} = \begin{pmatrix} \mathbf{1} & \mathbf{0} & \mathbf{0} \\ \mathbf{0} & \mathbf{1}^h \oplus \mathbf{X} & \mathbf{0} \\ \mathbf{0} & \mathbf{0} & \mathbf{1}^p \oplus \mathbf{X}^{-1} \end{pmatrix} \quad (52)$$

is identical to the G_0W_0 supermatrix formulation of Ref. 119, 123, 163–167, and results in the effective Hamiltonian \mathbf{H}^{GW} of Eq. (5). Here, $\mathbf{1}^h$ and $\mathbf{1}^p$ denote identity matrices defined over the 1h and 1p subspaces, respectively.

VIII. BEYOND-GW VERTEX CORRECTIONS FROM ECC

In our opinion, the newly established connection between the ECC formalism and the *GW* approximation opens exciting avenues for systematically including vertex corrections beyond *GW*. As noted at the end of Sec. II, vertex corrections can enter through three distinct components of the *GW* supermatrix [see Eq. (5)]: (i) the Fock matrix \mathbf{f} , (ii) the diagonal blocks \mathbf{C} , and (iii) the coupling blocks \mathbf{M} . Reformulating the building blocks \mathbf{C} and \mathbf{M} within the ECC framework [see Eq. (47)] provides direct access to vertex corrections that are positive semidefinite by construction, a notable advantage compared to vertex corrections derived from approximate solutions of Hedin's equations.^{149,154,156,159,160,162,181–187}

In this work, we explore corrections to \mathbf{f} through static Fock matrix corrections $\Sigma(\infty)$ as

$$\Sigma_{pq}(\infty) = \sum_{rs} \langle pq||rs \rangle (\gamma_{pr} - \gamma_{pr}^{\text{HF}}) \quad (53)$$

where $\langle pq||rs \rangle = \langle pq|rs \rangle - \langle pq|sr \rangle$, γ and γ^{HF} denote the correlated and HF one-body density matrices. Therefore, the augmented Fock matrix, used in the EOM treatment or, equivalently, in the *GW* supermatrix, reads

$$\mathbf{f} = \mathbf{f}^{\text{HF}} + \Sigma(\infty) \quad (54)$$

where \mathbf{f}^{HF} is the HF (or alternative mean-field) Fock matrix. Depending on the choice of γ , this modification allows for mimicking self-consistency effects^{188–190} (see Sec. IX), and/or additional vertex corrections beyond *GW*.

Beyond these static corrections, the ECC framework also enables the inclusion of missing exchange contributions in

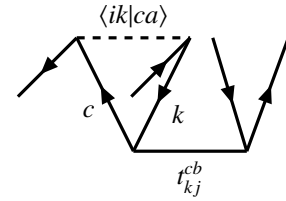
the matrices $\tilde{\mathbf{N}}$, \mathbf{N} , and \mathbf{D} , which enter \mathbf{H}^{EOM} [see Eq. (47)]. Here, we consider exchange-like contributions that arise from particle-hole contractions of the electron repulsion integrals $\langle pq|rs \rangle$ with the ECC amplitudes (\mathbf{t} and \mathbf{z}). The inclusion of such contributions shares similarity with the SOSEX ground-state energy correction to drCCD proposed in Ref. 191.

To illustrate how different exchange contributions can be included, we start investigating the diagrammatic representation of the following ring contraction between the electron repulsion integrals $\langle pq|rs \rangle$ with the ECC amplitude \mathbf{t}

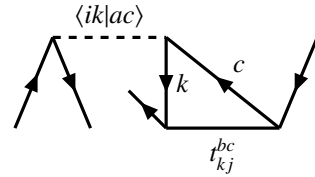
$$\begin{aligned} & \langle ik|ac \rangle \quad (55) \\ & \begin{array}{c} \text{a} \nearrow \text{i} \quad \text{k} \quad \text{c} \quad \text{j} \nearrow \text{b} \\ \text{---} \quad \text{---} \quad \text{---} \\ \text{---} \quad \text{---} \quad \text{---} \end{array} \\ & = \sum_{kc} \langle ik|ac \rangle t_{kj}^{cb} = \sum_{\lambda} B_{\nu\lambda} t_{\lambda\mu} \end{aligned}$$

entering the \mathbf{D} block of \mathbf{H}^{EOM} [see Eqs. (47) and (49)]. In this case, the particle and hole lines are connected to the same vertices of $\langle ik|ac \rangle$ and t_{kj}^{cb} . Three distinct exchange contributions can be identified by exchanging the vertices to which the particle and hole lines are connected:

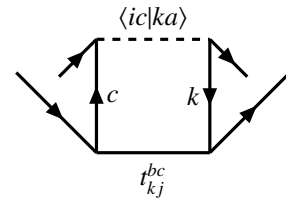
(i) Through connection to different vertices of the electron repulsion integral



(ii) Through connection to different vertices of the amplitude \mathbf{t}



and (iii) both

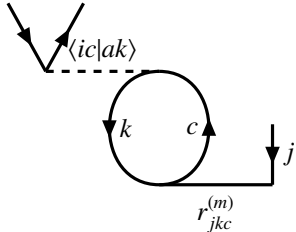


The latter can be identified as electron-hole-ladder/crossed-ring corrections.^{113,192} Additionally, we consider exchange

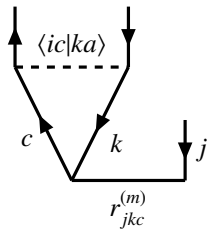
contributions in (i) originating from the contraction with the excitation vector \hat{R} (Sec. VI), i.e.,

$$\begin{aligned} \sum_{\nu} A_{\nu,\mu} r_{\mu j} &= \sum_{kc} A_{ia,kc} r_{jkc}^{(m)} \\ \rightarrow \sum_{kc} (A_{ia,kc} - \langle ic|ka \rangle) r_{jkc}^{(m)} \end{aligned} \quad (56)$$

The first term corresponds to the ring contraction



and the additional term in the last line represents the contraction of $\langle ic|ka \rangle$ with r_{jkc} , where the particle-hole indices (c and k) are located at different vertices of the electron repulsion integral:



This example contributes to \mathbf{D} [see Eq. (49)].

To explore the importance of the different exchange corrections, we have implemented the underlying working equations for (i), (ii), and (iii) in spin-adapted form for the EOM effective Hamiltonian of Eq. (47). The resulting equations can be found in the [Supplementary Material](#). In the following, we will denote the different exchange corrections as Γ_V^x for case (i), Γ_A^x for case (ii), and Γ_{CR}^x for case (iii). Combinations of these corrections will be indicated by the addition of the respective labels, e.g., Γ_{V+A}^x indicates the inclusion of both (i) and (ii) contributions.

We would like to stress that the proposed corrections (i) to (iii) are a choice made in the present work. The corrections are motivated also by their potential for low-scaling implementations. While the computational cost of the present approach is $\mathcal{O}(N^6)$, we would like to emphasize that the cost for determining the amplitudes can be reduced to $\mathcal{O}(N^4)$ through techniques such as Cholesky decomposition.^{112,165} Furthermore, in combination with the resolution-of-the-identity (RI) technique,^{193,194} the matrix-vector products for the EOM eigenvalue problem, including exchange corrections, can be reduced to $\mathcal{O}(N^5)$, whereas application of tensor-hypercontraction techniques (THC)^{195,196} reduces this scaling further to $\mathcal{O}(N^4)$. The applicability of these low-scaling techniques within the vertex corrections presented here will be explored in future work.

Beyond that, the choice made here can also be rationalized by comparison to alternative GW vertex corrections proposed

in the literature (see Refs. 149, 154, 156, 159, 160, 162, 181–187). Within Hedin’s equations [see Eqs. (1a)–(1e)], vertex correction enter both the self-energy Σ [see Eq. (1d)] and the polarizability P [see Eq. (1b)]. Note that the vertex itself is defined through the functional derivative of Σ with respect to G [see Eq. (1a)]. This formal structure has motivated a variety of practical schemes, commonly classified according to whether vertex corrections are included in Σ , in P , or in both. Moreover, different approximations to the vertex Γ have been explored,^{154,159,162,184,185} many of which suffer from the lack of positive semidefiniteness.^{160,187,197}

The choices made in the present work can be interpreted as modifying both Σ and P such that the resulting (non-Hermitian) self-energy remains positive semidefinite. However, several alternative, potentially systematically improvable, vertex corrections can be devised within the ECC framework, which we leave for future work. For example, of particular interest are the inclusion of additional contributions in the amplitude equations themselves and the effect of particle-particle and hole-hole ladder contributions at the EOM level.

IX. GW LINEARIZED DENSITY MATRIX FROM ECC PERTURBATION THEORY

As noted in Sec. VIII, the inclusion of static Fock matrix corrections $\Sigma(\infty)$ allows for mimicking self-consistency effects within the GW approximation. Here, we derive the GW linearized one-body density matrix γ within the ECC framework, which can be used to compute $\Sigma(\infty)$.

References 188–190 derived the linearized one-body density matrix within the GW approximation as

$$\gamma_{ij} = \delta_{ij} - \sum_{av} \frac{M_{ia,v} M_{ja,v}}{(\epsilon_i - \epsilon_a - \Omega_v)(\epsilon_j - \epsilon_a - \Omega_v)} \quad (57a)$$

$$\gamma_{ab} = \sum_{iv} \frac{M_{ai,v} M_{bi,v}}{(\epsilon_i - \epsilon_a - \Omega_v)(\epsilon_i - \epsilon_b - \Omega_v)} \quad (57b)$$

$$\begin{aligned} \gamma_{ia} &= \frac{f_{ia}}{\epsilon_i - \epsilon_a} \\ &+ \frac{1}{\epsilon_i - \epsilon_a} \left[\sum_{bv} \frac{M_{ib,v} M_{ab,v}}{\epsilon_i - \epsilon_b - \Omega_v} + \sum_{jv} \frac{M_{ij,v} M_{aj,v}}{\epsilon_j - \epsilon_a - \Omega_v} \right] \end{aligned} \quad (57c)$$

In the following, we show how these equations can be derived within the ECC framework perturbatively. For this, we partition the Hamiltonian as

$$\hat{H}(\lambda) = \hat{H}_0 + \lambda \hat{V} \quad (58)$$

where λ denotes the perturbation parameter, and

$$\hat{H}_0 = \sum_p f_{pp} \hat{a}_p^\dagger \hat{a}_p + \sum_{\mu\nu} \bar{A}_{\mu\nu} \hat{b}_\nu^\dagger \hat{b}_\mu \quad (59a)$$

$$\hat{V} = \sum_{pq\nu} \bar{M}_{pq\nu} \hat{a}_p^\dagger \hat{a}_q (\hat{b}_\nu^\dagger + \hat{b}_\nu) + \sum_{p \neq q} f_{pq} \hat{a}_p^\dagger \hat{a}_q \quad (59b)$$

Within perturbation theory,¹⁹⁸ the doubly similarity-transformed Hamiltonian reads

$$\tilde{H}(\lambda) = e^{\hat{Z}(\lambda)} e^{-\hat{T}(\lambda)} \hat{H}(\lambda) e^{\hat{T}(\lambda)} e^{-\hat{Z}(\lambda)} \quad (60)$$

where the excitation and deexcitation operators read

$$\hat{T}(\lambda) = \lambda \hat{T}^{(1)} + \lambda^2 \hat{T}^{(2)} + \dots \quad (61a)$$

$$\hat{Z}(\lambda) = \lambda \hat{Z}^{(1)} + \lambda^2 \hat{Z}^{(2)} + \dots \quad (61b)$$

with

$$\hat{T}^{(n)} = \hat{T}_1^{(n)} + \hat{T}_2^{(n)} = \sum_{ia} t_{ia}^{(n)} \hat{a}_a^\dagger \hat{a}_i + \sum_{iav} t_{iav}^{(n)} \hat{a}_a^\dagger \hat{a}_i \hat{b}_v^\dagger \quad (62a)$$

$$\hat{Z}^{(n)} = \hat{Z}_1^{(n)} + \hat{Z}_2^{(n)} = \sum_{ia} z_{ia}^{(n)} \hat{a}_i^\dagger \hat{a}_a + \sum_{iav} z_{iav}^{(n)} \hat{b}_v^\dagger \hat{a}_i^\dagger \hat{a}_a \quad (62b)$$

and the n th-order amplitude equations can be deduced from

$$\hat{T}_k^{(n)} \rightarrow \frac{1}{n!} \left. \frac{\partial^n \langle k | \bar{H}(\lambda) | 0 \rangle}{\partial \lambda^n} \right|_{\lambda=0} = 0 \quad (63a)$$

$$\hat{Z}_k^{(n)} \rightarrow \frac{1}{n!} \left. \frac{\partial^n \langle 0 | \bar{H}(\lambda) | k \rangle}{\partial \lambda^n} \right|_{\lambda=0} = 0 \quad (63b)$$

where $k \in \{1, 2\}$, $|1\rangle = \hat{a}_a^\dagger \hat{a}_i |0_e 0_B\rangle$, $|2\rangle = \hat{a}_a^\dagger \hat{a}_i \hat{b}_v^\dagger |0_e 0_B\rangle$, $\langle 1| = \langle |1\rangle|^\dagger$, $\langle 2| = \langle |2\rangle|^\dagger$, and $|0\rangle \equiv |0_e 0_B\rangle$ denotes the reference ground-state wave function.

Within the perturbative expansion, the n th-order contribution to the one-body density matrix is obtained from

$$\gamma_{pq}^{(n)} = \frac{\partial E^{(n)}}{\partial f_{pq}} \quad (64)$$

Under certain approximations, the first-order density matrix contributions of the occupied-occupied and virtual-virtual blocks is obtained from the second-order energy expression

$$E^{(2)} = \langle 0 | [\hat{V}, \hat{T}^{(1)}] + [\hat{Z}^{(1)}, \hat{V}] + [\hat{Z}^{(1)}, [\hat{H}_0, \hat{T}^{(1)}]] | 0 \rangle \quad (65)$$

The resulting density matrix blocks coincide with the linearized one-body GW density matrix [see Eqs. (57a) and (57b)] only when canonical Hartree–Fock orbitals are employed. If this is not the case, additional terms, due to non-zero amplitudes $t_{ia}^{(1)}$ and $z_{ia}^{(1)}$ have to be considered in these blocks as well. Furthermore, only the first term of the occupied-virtual block [see Eq. (57c)] is obtained at second-order, which is zero for canonical orbitals.

The additional terms of Eq. (57c) are recovered from a modified third-order energy expression

$$E^{(3)} = \langle 0 | [\hat{V}, \hat{T}_1^{(2)}] + [\hat{Z}_1^{(2)}, \hat{V}] | 0 \rangle \quad (66)$$

Note that the resulting density matrix is not symmetric, i.e., $\gamma_{pq} \neq \gamma_{qp}$, and is symmetrized throughout this work for convenience. The natural occupation numbers from the perturbative ECC treatment then coincide with those obtained from the linearized one-body GW density matrix, as reported in Eqs. (57a)–(57c). Complete spin-adapted working equations are provided in the [Supplementary Material](#).

X. COMPUTATIONAL DETAILS

All calculations were performed using a custom implementation built on the PySCF package.^{199,200} Unless otherwise stated,

G_0W_0 calculations were carried out without invoking the diagonal approximation, and all results employ Hartree–Fock as the mean-field starting point. The linearized GW density matrix was computed using the perturbative ECC framework described in Sec. IX. CCSD calculations were likewise performed with PySCF.^{199,200} The test set consists of 23 small molecules with accurate theoretical best estimates (TBEs) for inner- and outer-valence ionization potentials (IPs), taken from Ref. 201. All calculations employ the aug-cc-pVQZ basis set.^{202,203} We employ a large basis set to reduce basis set effects, thereby facilitating a more consistent, like-for-like comparison between the different schemes. The self-consistent field procedure is converged until the total energy changes by less than $10^{-9} E_h$. ECC amplitudes are iterated until the update satisfies $\|\Delta t\| < 10^{-8}$ and $\|\Delta z\| < 10^{-8}$. The Davidson solver used for computing G_0W_0 quasiparticle energies is converged to $10^{-8} E_h$.

XI. NUMERICAL RESULTS

First, we investigate the performance of various G_0W_0 vertex corrections, as proposed in Sec. VIII, for the calculation of the principal IPs (i.e., the lowest-energy IP of each system). The relative errors for these 23 principal IPs with respect to the reference TBE values for the benchmark set of Ref. 201 are displayed in Table I. The error distributions are visualized in the violin plots of Fig. 1.

In total, eight distinct G_0W_0 variants are considered. First, G_0W_0 IPs are computed within the diagonal approximation (as reported in Ref. 201), denoted as G_0W_0 (diag), as well as using the full self-energy, denoted as G_0W_0 (full). Furthermore, we consider G_0W_0 calculations including static Fock matrix corrections using the GW linearized density matrix (denoted as $+\gamma^{GW}$). Finally, we explore the effect of vertex corrections in \mathbf{H}^{EOM} : (i) Γ_V^x , (ii) Γ_A^x , and (iii) Γ_{CR}^x . For a motivation of these contributions, the reader is referred to Sec. VIII. Combinations of these vertex corrections are also considered and are denoted as, for example, Γ_{V+A}^x , corresponding to $\Gamma_V^x + \Gamma_A^x$. Vertex corrections are also considered in combination with static Fock matrix corrections.

Overall, similar errors in the principal IPs are observed for both G_0W_0 (diag) and G_0W_0 (full), with mean absolute errors (MAEs) of 0.423 eV and 0.420 eV, respectively. In general, the IPs for G_0W_0 (diag) and G_0W_0 (full) in combination with the Hartree–Fock starting point are systematically overestimated when compared to the TBEs. This is a known issue for G_0W_0 ,^{90,159,204–207} and by performing full self-consistency, the IPs are known to be lowered.^{90,159,204–206} We observe a similar trend here, where the inclusion of static Fock matrix corrections based on the GW linearized density matrix lowers the IPs, resulting in a MAE of 0.167 eV.

Including a combination of all three vertex corrections, Γ_{V+A+CR}^x , does only slightly improve the results, compared to G_0W_0 , and yields a MAE of 0.420 eV. However, when combined with static Fock matrix corrections, the MAE is significantly reduced. While all variants including vertex corrections in combination with static Fock matrix corrections

($+\Gamma_V^x + \gamma^{GW}$, $+\Gamma_A^x + \gamma^{GW}$, $+\Gamma_{V+A}^x + \gamma^{GW}$, $+\Gamma_{V+A+CR}^x + \gamma^{GW}$) result in improvements when compared to $G_0W_0 + \gamma^{GW}$, the best performance is obtained when Γ_V^x is considered. In this case one finds a MAE of 0.082 eV, and a mean-signed error (MSE) of -0.011 eV, which is even better than the MAE of 0.098 eV and MSE of -0.053 eV obtained from EOM-IP-CCSD. All variants lower the magnitude of the IPs slightly further when compared to $G_0W_0 + \gamma^{GW}$, while also reducing the spread of the errors.

A direct comparison between the present results and previously proposed vertex corrections for molecular IPs is challenging. The available studies differ in several important aspects, including the molecular test sets considered,^{159,184,187} the underlying mean-field starting points,¹⁸² as well as the basis sets and other numerical settings employed.^{154,184} Even qualitative trends are difficult to establish: while some vertex-corrected schemes systematically decrease IPs,^{162,184,207} others lead to an overall increase.^{159,182} Consequently, it is not straightforward to provide a definitive assessment of the present vertex corrections relative to alternative approaches. Nevertheless, we emphasize that the vertex corrections introduced here lead to a clear and significant improvement in the description of principal IPs.

Next, we assess the performance of the different G_0W_0 variants for the second IPs. The error distributions are visualized in the violin plots of Fig. 2, and the relative errors are displayed in Table II. For the second IPs, we observe overall similar trends as for the principal IPs. While G_0W_0 (diag) and G_0W_0 (full) yield similar MAEs of 0.474 eV and 0.466 eV, the inclusion of static Fock matrix corrections through the GW linearized density reduces the MAE to 0.308 eV. Notably, all vertex corrections in combination with γ^{GW} yield significant improvements of more than 0.7 eV when compared to $G_0W_0 + \gamma^{GW}$. The best overall performance is achieved with $+\Gamma_{V+A+CR}^x + \gamma^{GW}$, resulting in a MAE of 0.183 eV, only slightly higher than the MAE of 0.157 eV obtained from EOM-IP-CCSD. Moreover, the corresponding MSE of 0.035 eV is lower than the MSE of 0.099 eV obtained for EOM-IP-CCSD. In all cases, the largest outlier is for Argon. Given the large reference TBE value for the second IP (29.182 eV), the relative error of 2.48 % for EOM-IP-CCSD and 3.69 % for $G_0W_0 + \Gamma_{V+A+CR}^x + \gamma^{GW}$ is relatively small compared to the absolute error of 0.725 eV and 1.078 eV, respectively.

XII. CONCLUSION

In summary, we have established a formal connection between the extended direct ring coupled cluster doubles (ECCD) framework and the G_0W_0 approximation. When applied to the electron-boson Hamiltonian in combination with the equation-of-motion formalism, this procedure recovers the G_0W_0 quasiparticle energies exactly. Furthermore, we have derived the linearized one-body GW density matrix within the ECC framework using perturbation theory. Exploiting the established connection between ECC and GW , we have proposed several vertex corrections beyond GW that can be systematically included within the ECC framework, while keeping positive

semi-definiteness in the corresponding self-energy. Preliminary numerical results for a benchmark set of 23 small molecules demonstrate the potential of the proposed vertex corrections to significantly improve the accuracy of G_0W_0 ionization potentials. Overall, the present work opens exciting avenues for including vertex corrections beyond GW within the ECC framework, such as the inclusion of particle-particle and hole-hole ladder contributions.

ACKNOWLEDGMENTS

The authors would like to thank Antoine Marie for insightful discussions. This project has received funding from the European Research Council (ERC) under the European Union's Horizon 2020 research and innovation programme (Grant agreement No. 863481). J. T. acknowledges funding from the Fonds der Chemischen Industrie (FCI) via a Liebig fellowship and support by the Cluster of Excellence "CUI: Advanced Imaging of Matter" of the Deutsche Forschungsgemeinschaft (DFG) (EXC 2056, funding ID 390715994). For this work, the HPC-cluster Hummel-2 at the University of Hamburg was used. The cluster was funded by Deutsche Forschungsgemeinschaft (DFG, German Research Foundation) - 498394658. Support and funding from the European Research Council (ERC) (Grant Agreement No. 101087184) is gratefully acknowledged.

DATA AVAILABILITY STATEMENT

The data that supports the findings of this study are available within the article and its supplementary material.

REFERENCES

- T. D. Crawford and H. F. Schaefer, "An Introduction to Coupled Cluster Theory for Computational Chemists," in *Reviews in Computational Chemistry* (John Wiley & Sons, Ltd, 2000) pp. 33–136.
- P. Piecuch, K. Kowalski, I. S. O. Pimienta, and M. J. McGuire, "Recent advances in electronic structure theory: Method of moments of coupled-cluster equations and renormalized coupled-cluster approaches," *Int. Rev. Phys. Chem.* **21**, 527–655 (2002).
- R. J. Bartlett and M. Musial, "Coupled-cluster theory in quantum chemistry," *Rev. Mod. Phys.* **79**, 291–352 (2007).
- I. Shavitt and R. J. Bartlett, *Many-Body Methods in Chemistry and Physics: MBPT and Coupled-Cluster Theory*, Cambridge Molecular Science (Cambridge University Press, Cambridge, 2009).
- R. J. Bartlett, "Perspective on coupled-cluster theory. the evolution toward simplicity in quantum chemistry," *Phys. Chem. Chem. Phys.* **26**, 8013–8037 (2024).
- D. J. Rowe, "Equations-of-Motion Method and the Extended Shell Model," *Rev. Mod. Phys.* **40**, 153–166 (1968).
- H. Koch, H. J. A. Jensen, P. Jorgensen, and T. Helgaker, "Excitation energies from the coupled cluster singles and doubles linear response function (CCSDLR). Applications to Be, CH⁺, CO, and H₂O," *J. Chem. Phys.* **93**, 3345–3350 (1990).
- J. F. Stanton and R. J. Bartlett, "The equation of motion coupled-cluster method. a systematic biorthogonal approach to molecular excitation energies, transition probabilities, and excited state properties," *J. Chem. Phys.* **98**, 7029–7039 (1993).

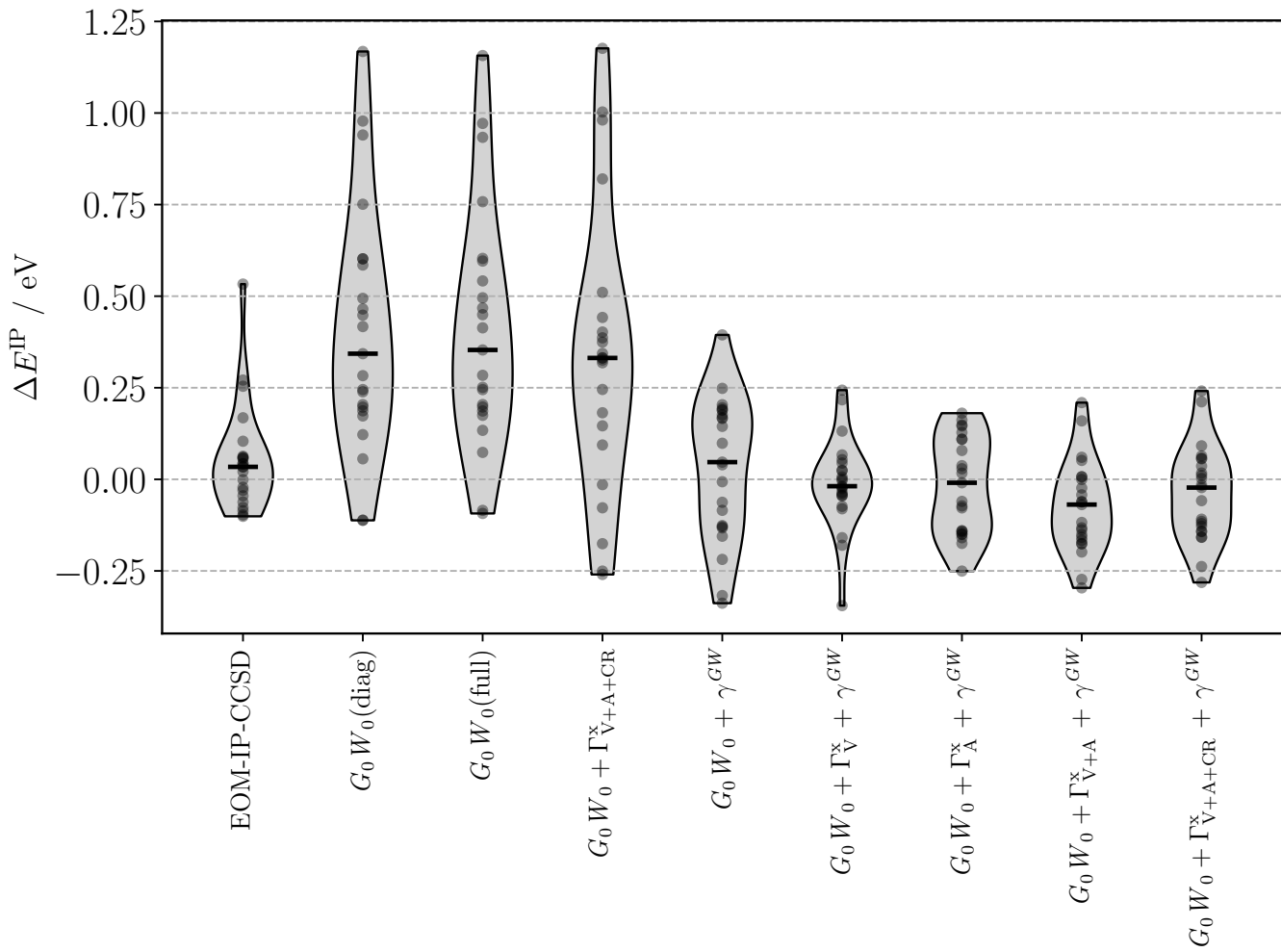


FIG. 1. Violin plots of the errors (in eV) for the principal IPs obtained with various G_0W_0 variants and EOM-IP-CCSD with respect to the TBEs for the benchmark set of 23 molecular systems from Ref. 201 computed with the aug-cc-pVQZ basis. Note that $\Gamma_{V+A}^x = \Gamma_V^x + \Gamma_A^x$ and $\Gamma_{V+A+CR}^x = \Gamma_{V+A}^x + \Gamma_{CR}^x$.

- ⁹H. Koch, R. Kobayashi, A. Sanchez de Merás, and P. Jorgensen, “Calculation of size-intensive transition moments from the coupled cluster singles and doubles linear response function,” *J. Chem. Phys.* **100**, 4393–4400 (1994).
- ¹⁰K. Sneskov and O. Christiansen, “Excited state coupled cluster methods,” *WIREs Comput. Mol. Sci.* **2**, 566–584 (2012).
- ¹¹A. Tajti, P. G. Szalay, A. G. Császár, M. Kállay, J. Gauss, E. F. Valeev, B. A. Flowers, J. Vázquez, and J. F. Stanton, “Heat: High accuracy extrapolated ab initio thermochemistry,” *J. Chem. Phys.* **121**, 11599–11613 (2004).
- ¹²Y. J. Bomble, J. Vázquez, M. Kállay, C. Michaux, P. G. Szalay, A. G. Császár, J. Gauss, and J. F. Stanton, “High-accuracy extrapolated ab initio thermochemistry. ii. minor improvements to the protocol and a vital simplification,” *J. Chem. Phys.* **125**, 064108 (2006).
- ¹³M. E. Harding, J. Vazquez, B. Ruscic, A. K. Wilson, J. Gauss, and J. F. Stanton, “High-accuracy extrapolated ab initio thermochemistry. iii. additional improvements and overview,” *J. Chem. Phys.* **128**, 114111 (2008).
- ¹⁴A. Karton, E. Rabinovich, J. M. L. Martin, and B. Ruscic, “W4 theory for computational thermochemistry: In pursuit of confident sub-kJ/mol predictions,” *J. Chem. Phys.* **125**, 144108 (2006).
- ¹⁵A. Karton, N. Sylvestsky, and J. M. L. Martin, “W4-17: A diverse and high-confidence dataset of atomization energies for benchmarking high-level electronic structure methods,” *J. Comput. Chem.* **38**, 2063–2075 (2017).
- ¹⁶L. Goerigk and S. Grimme, “A thorough benchmark of density functional methods for general main group thermochemistry, kinetics, and noncovalent interactions,” *Phys. Chem. Chem. Phys.* **13**, 6670–6688 (2011).
- ¹⁷L. Goerigk and S. Grimme, “Efficient and accurate double-hybrid-meta-gga density functionals—evaluation with the extended gmtkn30 database for general main group thermochemistry, kinetics, and noncovalent interactions,” *J. Chem. Theory Comput.* **7**, 291–309 (2011).
- ¹⁸L. Goerigk, A. Hansen, C. Bauer, S. Ehrlich, A. Najibi, and S. Grimme, “A look at the density functional theory zoo with the advanced gmtkn55 database for general main group thermochemistry, kinetics and noncovalent interactions,” *Phys. Chem. Chem. Phys.* **19**, 32184–32215 (2017).
- ¹⁹P.-F. Loos, A. Scemama, and D. Jacquemin, “The quest for highly accurate excitation energies: A computational perspective,” *J. Phys. Chem. Lett.* **11**, 2374–2383 (2020).
- ²⁰M. Véril, A. Scemama, M. Caffarel, F. Lipparini, M. Boggio-Pasqua, D. Jacquemin, and P.-F. Loos, “Questdb: A database of highly accurate excitation energies for the electronic structure community,” *WIREs Comput. Mol. Sci.* **11**, e1517 (2021).
- ²¹P.-F. Loos, M. Boggio-Pasqua, A. Blondel, F. Lipparini, and D. Jacquemin, “Quest database of highly-accurate excitation energies,” *J. Chem. Theory Comput.* **21**, 8010–8033 (2025).
- ²²J. Hubbard, “The description of collective motions in terms of many-body perturbation theory,” *Proc. R. Soc. Lond. A* **240**, 539–560 (1957).

TABLE I. Errors (in eV) of the principal IPs with respect to the TBEs for the benchmark set of 23 molecular systems from Ref. 201 computed using various G_0W_0 variants with the aug-cc-pVQZ basis.

Mol.	CCSD ^a	G_0W_0 variants						
		(diag) ^b	(full)	$+\Gamma_{A+V+CR}^x$	$+\gamma^{GW}$	$+\Gamma_V^x + \gamma^{GW}$	$\Gamma_A^x + \gamma^{GW}$	$+\Gamma_{V+A}^x + \gamma^{GW}$
H ₂ S	0.034	0.204	0.204	0.375	-0.155	-0.040	-0.150	-0.042
CS	0.254	1.168	1.157	1.177	0.166	0.217	0.128	0.16
BeO	-0.077	-0.111	-0.085	-0.251	0.040	-0.019	-0.072	-0.151
CH ₄	0.021	0.465	0.468	0.318	-0.007	-0.159	-0.009	-0.176
C ₂	0.533	0.585	0.596	1.003	-0.338	-0.180	-0.159	0.007
BN	-0.001	-0.112	-0.093	-0.015	-0.317	-0.345	-0.250	-0.273
Ne	-0.101	0.122	0.134	-0.176	0.195	0.054	0.037	-0.132
HF	-0.097	0.239	0.251	-0.078	0.188	0.025	0.029	-0.167
CO ₂	0.056	0.602	0.603	0.442	0.145	0.024	0.079	-0.069
LiF	-0.045	0.056	0.074	-0.260	0.190	0.044	0.017	-0.158
HCl	0.042	0.197	0.197	0.332	-0.133	-0.045	-0.140	-0.062
CH ₂ O	-0.030	0.602	0.542	0.182	0.248	-0.003	0.146	-0.138
Ar	0.063	0.187	0.187	0.326	-0.129	-0.036	-0.144	-0.061
SiH ₄	0.059	0.494	0.496	0.386	0.176	0.067	0.181	0.060
BH ₃	0.043	0.448	0.449	0.331	0.098	-0.025	0.109	-0.024
H ₂ O	-0.062	0.343	0.353	0.146	0.047	-0.045	-0.078	-0.198
N ₃	-0.022	0.417	0.414	0.344	-0.063	-0.074	-0.141	-0.176
BF	0.104	0.245	0.245	0.510	-0.219	0.001	-0.175	0.052
LiCl	0.060	0.173	0.175	0.245	-0.126	-0.080	-0.150	-0.118
CO	0.271	0.940	0.934	0.981	0.168	0.243	0.148	0.209
F ₂	-0.086	0.751	0.758	0.094	0.394	0.007	0.162	-0.296
P ₃	0.034	0.283	0.284	0.402	-0.085	-0.021	-0.060	-0.000
N ₂	0.168	0.978	0.972	0.820	0.204	0.132	0.110	0.007
MAE	0.098	0.423	0.420	0.400	0.167	0.082	0.116	0.119
MSE	0.053	0.403	0.405	0.332	0.030	-0.011	-0.017	-0.076
								-0.039

^a EOM-IP-CCSD data taken from Ref. 201.

^b G_0W_0 results computed within the diagonal approximation taken from Ref. 201.

TABLE II. Errors (in eV) of the second IPs with respect to the TBEs for the benchmark set of 23 molecular systems from Ref. 201 computed using various G_0W_0 variants with the aug-cc-pVQZ basis.

Mol.	CCSD ^a	G_0W_0 variants						
		(diag) ^b	(full)	$+\Gamma_{A+V+CR}^x$	$+\gamma^{GW}$	$+\Gamma_V^x + \gamma^{GW}$	$\Gamma_A^x + \gamma^{GW}$	$+\Gamma_{V+A}^x + \gamma^{GW}$
CS	0.037	0.298	0.296	0.362	-0.076	-0.060	-0.065	-0.058
BeO	0.123	-0.413	0.141	0.449	-0.309	-0.168	-0.234	-0.099
CH ₄	-0.033	0.085	0.095	-0.369	0.283	0.033	0.082	-0.181
C ₂	0.278	0.84	0.842	0.728	0.297	0.289	0.193	0.159
BN	0.013	-0.117	-0.080	0.258	-0.402	-0.134	-0.386	-0.160
Ne	0.154	-0.255	-0.241	0.035	-0.182	0.350	-0.448	0.084
HF	-0.081	0.157	0.144	-0.080	0.067	-0.070	-0.019	-0.176
CO ₂	0.462	1.079	1.125	1.110	0.559	0.578	0.497	0.489
LiF	-0.039	0.121	0.134	-0.351	0.277	-0.006	0.097	-0.216
HCl	0.054	0.303	0.297	0.358	-0.063	-0.057	-0.056	-0.060
CH ₂ O	0.049	0.141	0.162	0.153	-0.193	-0.243	-0.166	-0.238
Ar	0.725	2.042	2.042	1.496	1.685	1.268	1.500	1.067
SiH ₄	0.247	0.839	0.845	0.787	0.521	0.516	0.476	0.436
BH ₃	0.096	0.448	0.453	0.434	0.077	0.094	0.050	0.042
H ₂ O	-0.067	0.323	0.309	0.099	0.025	-0.088	-0.079	-0.217
N ₃	0.000	0.368	0.372	0.142	-0.061	-0.279	-0.077	-0.313
BF	-0.418	0.285	0.302	0.165	0.277	0.137	0.138	0.004
LiCl	0.061	0.201	0.202	0.231	-0.105	-0.101	-0.128	-0.137
CO	0.075	0.244	0.263	0.289	-0.034	-0.062	-0.036	-0.084
F ₂	0.104	1.161	1.181	0.274	0.843	0.326	0.569	-0.043
PH ₃	0.041	0.43	0.432	0.375	0.048	-0.035	0.056	-0.038
N ₂	0.306	0.278	0.286	0.546	-0.385	-0.314	-0.266	-0.197
MAE	0.157	0.461	0.466	0.413	0.308	0.237	0.255	0.204
MSE	0.099	0.427	0.437	0.341	0.143	0.090	0.077	0.001
								0.035

^a EOM-IP-CCSD data taken from Ref. 201.

^b G_0W_0 results computed within the diagonal approximation taken from Ref. 201.

²³F. Coester, “Bound states of a many-particle system,” *Nuc. Phys.* **7**, 421–424 (1958).

²⁴F. Coester and H. Kümmel, “Short-range correlations in nuclear wave functions,” *Nuclear Physics* **17**, 477–485 (1960).

²⁵O. Sinanoglu, “Many-electron theory of atoms and molecules. i. shells, electron pairs vs many-electron correlations,” *J. Chem. Phys.* **36**, 706–717 (1962).

²⁶J. Čížek, “On the Correlation Problem in Atomic and Molecular Systems. Calculation of Wavefunction Components in Ursell-Type Expansion Using Quantum-Field Theoretical Methods,” *J. Chem. Phys.* **45**, 4256–4266 (1966).

²⁷J. Paldus, J. Čížek, and I. Shavitt, “Correlation problems in atomic and molecular systems. iv. extended coupled-pair many-electron theory and its application to the bh_3 molecule,” *Phys. Rev. A* **5**, 50–67 (1972).

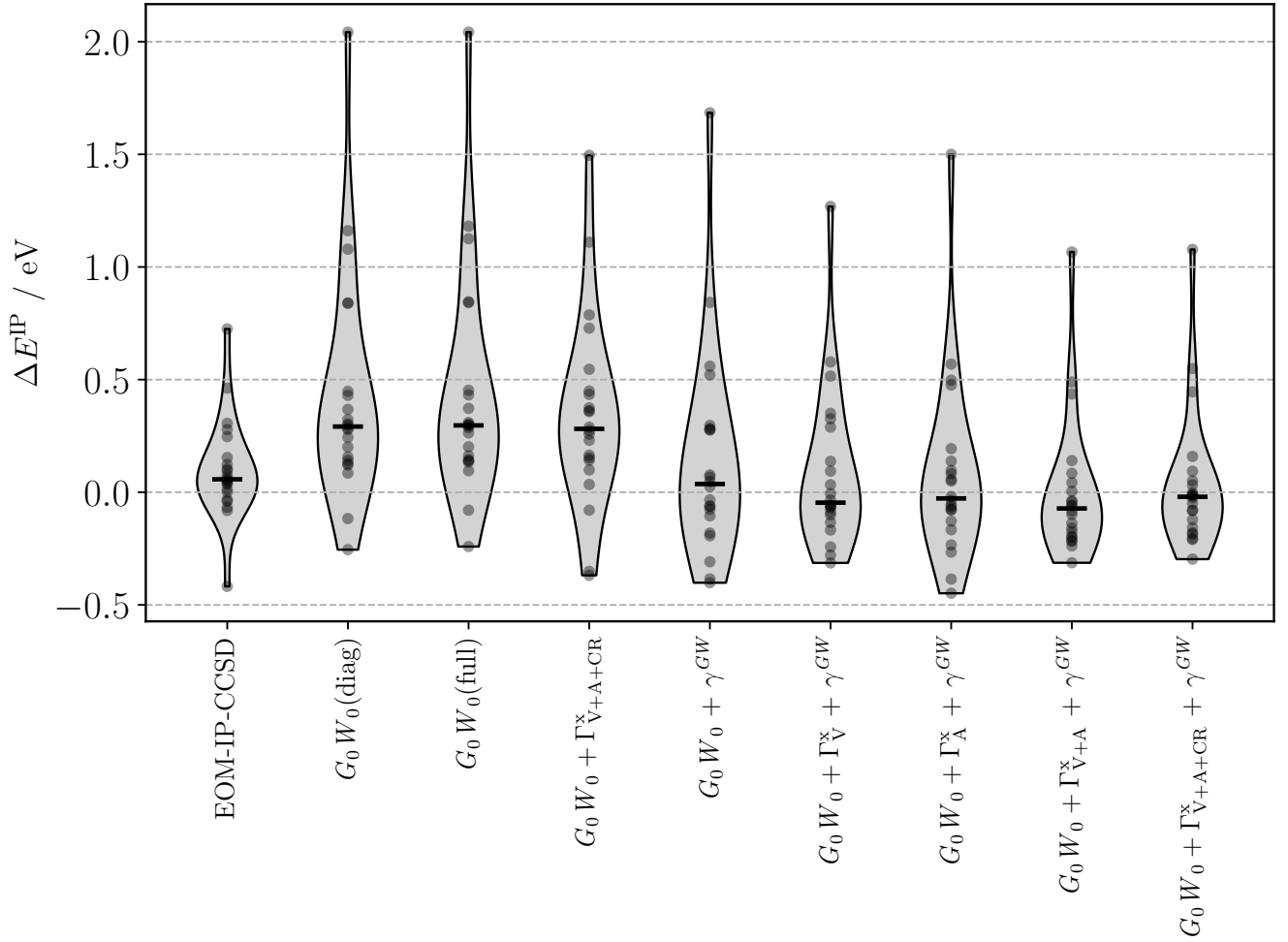


FIG. 2. Violin plots of the errors (in eV) for the second IPs obtained with various G_0W_0 variants and EOM-IP-CCSD with respect to the TBEs for the benchmark set of 23 molecular systems from Ref. 201 computed with the aug-cc-pVQZ basis. Note that $\Gamma_{V+A}^x = \Gamma_V^x + \Gamma_A^x$ and $\Gamma_{V+A+CR}^x = \Gamma_{V+A}^x + \Gamma_{CR}^x$.

- ²⁸R. F. Bishop, “An overview of coupled cluster theory and its applications in physics,” *Theor. Chem. Acc.* **80**, 95–148 (1991).
- ²⁹D. J. Dean and M. Hjorth-Jensen, “Coupled-cluster approach to nuclear physics,” *Phys. Rev. C* **69**, 054320 (2004).
- ³⁰K. Kowalski, D. J. Dean, M. Hjorth-Jensen, T. Papenbrock, and P. Piecuch, “Coupled cluster calculations of ground and excited states of nuclei,” *Phys. Rev. Lett.* **92**, 132501 (2004).
- ³¹G. Hagen, T. Papenbrock, M. Hjorth-Jensen, and D. J. Dean, “Coupled-cluster computations of atomic nuclei,” *Rep. Prog. Phys.* **77**, 096302 (2014).
- ³²T. Gruber, K. Liao, T. Tsatsoulis, F. Hummel, and A. Grüneis, “Applying the coupled-cluster ansatz to solids and surfaces in the thermodynamic limit,” *Phys. Rev. X* **8**, 021043 (2018).
- ³³I. Y. Zhang and A. Grüneis, “Coupled cluster theory in materials science,” *Front. Mat.* **6**, 123 (2019).
- ³⁴X. Wang and T. C. Berkelbach, “Excitons in solids from periodic equation-of-motion coupled-cluster theory,” *J. Chem. Theory Comput.* **16**, 3095–3103 (2020).
- ³⁵V. A. Neufeld and T. C. Berkelbach, “Highly accurate electronic structure of metallic solids from coupled-cluster theory with nonperturbative triple excitations,” *Phys. Rev. Lett.* **131**, 186402 (2023).
- ³⁶N. Masić, A. Irmler, T. Schäfer, and A. Grüneis, “Averting the infrared catastrophe in the gold standard of quantum chemistry,” *Phys. Rev. Lett.* **131**, 186401 (2023).
- ³⁷H.-Z. Ye and T. C. Berkelbach, “Periodic local coupled-cluster theory for insulators and metals,” *J. Chem. Theory Comput.* **20**, 8948–8959 (2024).
- ³⁸E. A. Vo, X. Wang, and T. C. Berkelbach, “Performance of periodic eom-ccsd for bandgaps of inorganic semiconductors and insulators,” *J. Chem. Phys.* **160**, 044106 (2024).
- ³⁹E. Moerman, A. Gallo, A. Irmler, T. Schäfer, F. Hummel, A. Grüneis, and M. Scheffler, “Finite-size effects in periodic eom-ccsd for ionization energies and electron affinities: Convergence rate and extrapolation to the thermodynamic limit,” *J. Chem. Theory Comput.* **21**, 1865–1878 (2025).
- ⁴⁰E. Moerman, H. Miranda, A. Gallo, A. Irmler, T. Schäfer, F. Hummel, M. Engel, G. Kresse, M. Scheffler, and A. Grüneis, “Exploring the accuracy of the equation-of-motion coupled-cluster band gap of solids,” *Phys. Rev. B* **111**, L121202 (2025).
- ⁴¹G. P. Purvis III and R. J. Bartlett, “A full coupled-cluster singles and doubles model: The inclusion of disconnected triples,” *J. Chem. Phys.* **76**, 1910–1918 (1982).
- ⁴²K. Raghavachari, G. W. Trucks, J. A. Pople, and M. Head-Gordon, “A fifth-order perturbation comparison of electron correlation theories,” *Chem. Phys. Lett.* **157**, 479–483 (1989).
- ⁴³J. Bomble, J. F. Stanton, M. Kállay, and J. Gauss, “Coupled-cluster methods including noniterative corrections for quadruple excitations,” *J. Chem. Phys.* **123**, 054101 (2005).

- ⁴⁴M. Kodrycka and K. Patkowski, "Platinum, gold, and silver standards of intermolecular interaction energy calculations," *J. Chem. Phys.* **151**, 070901 (2019).
- ⁴⁵T. Helgaker and P. Jørgensen, "Analytical calculation of geometrical derivatives in molecular electronic structure theory," (Academic Press, 1988) pp. 183–245.
- ⁴⁶H. Koch, H. J. Aa. Jensen, P. Jørgensen, T. Helgaker, G. E. Scuseria, and H. F. Schaefer, "Coupled cluster energy derivatives. Analytic Hessian for the closed-shell coupled cluster singles and doubles wave function: Theory and applications," *J. Chem. Phys.* **92**, 4924–4940 (1990).
- ⁴⁷H. Koch and P. Jørgensen, "Coupled cluster response functions," *J. Chem. Phys.* **93**, 3333–3344 (1990).
- ⁴⁸T. Helgaker and P. Jørgensen, "Calculation of geometrical derivatives in molecular electronic structure theory," in *Methods in Computational Molecular Physics*, edited by S. Wilson and G. H. F. Diercksen (Springer US, Boston, MA, 1992) pp. 353–421.
- ⁴⁹J. Gauss, "Molecular properties," in *Modern Methods and Algorithms of Quantum Chemistry*, edited by J. Grotendorst (John von Neumann Institute for Computing, 2000) pp. 541–592.
- ⁵⁰T. Helgaker, P. Jørgensen, and J. Olsen, *Molecular Electronic-Structure Theory* (John Wiley & Sons, Inc., 2013).
- ⁵¹F. Hampe and S. Stopkowicz, "Transition-dipole moments for electronic excitations in strong magnetic fields using equation-of-motion and linear response coupled-cluster theory," *J. Chem. Theory Comput.* **15**, 4036–4043 (2019).
- ⁵²M. Musial, S. A. Kucharski, and R. J. Bartlett, "Equation-of-motion coupled cluster method with full inclusion of the connected triple excitations for ionized states: Ip-eom-ccsd," *J. Chem. Phys.* **118**, 1128–1136 (2003).
- ⁵³M. Musial and R. J. Bartlett, "Equation-of-motion coupled cluster method with full inclusion of connected triple excitations for electron-attached states: Ea-eom-ccsd," *J. Chem. Phys.* **119**, 1901–1908 (2003).
- ⁵⁴A. I. Krylov, "Equation-of-motion coupled-cluster methods for open-shell and electronically excited species: The hitchhiker's guide to fock space," *Annu. Rev. Phys. Chem.* **59**, 433–462 (2008).
- ⁵⁵J. Shen and P. Piecuch, "Doubly electron-attached and doubly ionized equation-of-motion coupled-cluster methods with 4-particle–2-hole and 4-hole–2-particle excitations and their active-space extensions," *J. Chem. Phys.* **138**, 194102 (2013).
- ⁵⁶S. Gulania, T.-C. Jagau, and A. I. Krylov, "Eom-cc guide to fock-space travel: the c2 edition," *Faraday Discuss.* **217**, 514–532 (2019).
- ⁵⁷M. Musial and R. J. Bartlett, "Multireference Fock-space coupled-cluster and equation-of-motion coupled-cluster theories: The detailed interconnections," *J. Chem. Phys.* **129**, 134105 (2008).
- ⁵⁸M. Musial, A. Perera, and R. J. Bartlett, "Multireference coupled-cluster theory: The easy way," *J. Chem. Phys.* **134**, 114108 (2011).
- ⁵⁹D. I. Lyakh, M. Musial, V. F. Lotrich, and R. J. Bartlett, "Multireference nature of chemistry: The coupled-cluster view," *Chem. Rev.* **112**, 182–243 (2012).
- ⁶⁰A. Kohn, M. Hanauer, L. A. Mück, T.-C. Jagau, and J. Gauss, "State-specific multireference coupled-cluster theory," *WIREs Comput. Mol. Sci.* **3**, 176–197 (2013).
- ⁶¹A. I. Krylov, "The quantum chemistry of open-shell species," in *Reviews in Computational Chemistry*, edited by A. L. Parrill and K. B. Lipkowitz (John Wiley & Sons, Ltd, 2017) pp. 151–224.
- ⁶²F. A. Evangelista, "Perspective: Multireference coupled cluster theories of dynamical electron correlation," *J. Chem. Phys.* **149**, 030901 (2018).
- ⁶³G. Onida, L. Reining, and A. Rubio, "Electronic excitations: Density-functional versus many-body green's function approaches," *Rev. Mod. Phys.* **74**, 601–659 (2002).
- ⁶⁴R. M. Martin, L. Reining, and D. M. Ceperley, *Interacting Electrons: Theory and Computational Approaches* (Cambridge University Press, 2016).
- ⁶⁵E. E. Salpeter and H. A. Bethe, "A relativistic equation for bound-state problems," *Phys. Rev.* **84**, 1232 (1951).
- ⁶⁶L. Hedin, "New method for calculating the one-particle Green's function with application to the electron-gas problem," *Phys. Rev.* **139**, A796 (1965).
- ⁶⁷F. Aryasetiawan and O. Gunnarsson, "The gw method," *Rep. Prog. Phys.* **61**, 237–312 (1998).
- ⁶⁸L. Reining, "The GW approximation: Content, successes and limitations: The GW approximation," *Wiley Interdiscip. Rev. Comput. Mol. Sci.* **8**, e1344 (2017).
- ⁶⁹B. I. Lundqvist, "Single-particle spectrum of the degenerate electron gas: Ii. numerical results for electrons coupled to plasmons," *Physik der Kondensierten Materie* **6**, 206–217 (1967).
- ⁷⁰B. I. Lundqvist, "Single-particle spectrum of the degenerate electron gas: I. the structure of the spectral weight function," *Physik der Kondensierten Materie* **6**, 193–205 (1967).
- ⁷¹G. D. Mahan and B. E. Sernelius, "Electron-electron interactions and the bandwidth of metals," *Phys. Rev. Lett.* **62**, 2718 (1989).
- ⁷²G. Strinati, H. J. Mattausch, and W. Hanke, "Dynamical aspects of correlation corrections in a covalent crystal," *Phys. Rev. B* **25**, 2867–2888 (1982).
- ⁷³G. Strinati, "Dynamical shift and broadening of core excitons in semiconductors," *Phys. Rev. Lett.* **49**, 1519 (1982).
- ⁷⁴M. S. Hybertsen and S. G. Louie, "First-principles theory of quasiparticles: Calculation of band gaps in semiconductors and insulators," *Phys. Rev. Lett.* **55**, 1418 (1985).
- ⁷⁵M. S. Hybertsen and S. G. Louie, "Electron correlation in semiconductors and insulators: Band gaps and quasiparticle energies," *Phys. Rev. B* **34**, 5390–5413 (1986).
- ⁷⁶R. W. Godby, M. Schlüter, and L. J. Sham, "Accurate Exchange-Correlation Potential for Silicon and Its Discontinuity on Addition of an Electron," *Phys. Rev. Lett.* **56**, 2415–2418 (1986).
- ⁷⁷R. W. Godby, M. Schlüter, and L. J. Sham, "Quasiparticle energies in GaAs and AlAs," *Phys. Rev. B* **35**, 4170–4171 (1987).
- ⁷⁸J. Schirmer, *Many-Body Methods for Atoms, Molecules and Clusters* (Springer, 2018).
- ⁷⁹A. Dreuw, A. Papapostolou, and A. L. Dempwolff, "Algebraic diagrammatic construction schemes employing the intermediate state formalism: Theory, capabilities, and interpretation," *J. Phys. Chem. A* **127**, 6635–6646 (2023).
- ⁸⁰L. Cederbaum, "Application of Green's functions to excitations accompanying photoionization in atoms and molecules," *Mol. Phys.* **28**, 479–493 (1974).
- ⁸¹J. Schirmer, L. S. Cederbaum, W. Domcke, and W. von Niessen, "Strong Correlation Effects in inner Valence Ionization of N2 AND CO," *Chem. Phys.* **26**, 149–153 (1977).
- ⁸²L. S. Cederbaum, J. Schirmer, W. Domcke, and W. von Niessen, "Complete breakdown of the quasiparticle picture for inner valence electrons," *J. Phys. B: At. Mol. Phys.* **10**, L549 (1977).
- ⁸³W. von Niessen, L. S. Cederbaum, and W. Domcke, "On green's function methods for the study of ionic states in atoms and molecules," in *Excited States in Quantum Chemistry: Theoretical and Experimental Aspects of the Electronic Structure and Properties of the Excited States in Atoms, Molecules and Solids*, edited by C. A. Nicolaides and D. R. Beck (Springer Netherlands, Dordrecht, 1979) pp. 183–272.
- ⁸⁴L. S. Cederbaum, W. Domcke, J. Schirmer, and W. von Niessen, "Many-Body Effects in Valence and Core Photoionization of Molecules," *Phys. Scr.* **21**, 481 (1980).
- ⁸⁵W. Von Niessen, L. S. Cederbaum, W. Domcke, and G. H. F. Diercksen, "Green's function calculations on the complete valence ionization spectra of HF, HCl, HBr AND HI," *Chem. Phys.* **56**, 43–52 (1981).
- ⁸⁶W. von Niessen, J. Schirmer, and L. Cederbaum, "Computational methods for the one-particle green's function," *Comput. Phys. Rep.* **1**, 57–125 (1984).
- ⁸⁷L. S. Cederbaum, "On green's functions and their applications," *Int. J. Quantum Chem.* **38**, 393–404 (1990).
- ⁸⁸E. L. Shirley and R. M. Martin, "Gw quasiparticle calculations in atoms," *Phys. Rev. B* **47**, 15404–15412 (1993).
- ⁸⁹M. Rohlffing and S. G. Louie, "Electron-hole excitations and optical spectra from first principles," *Phys. Rev. B* **62**, 4927–4944 (2000).
- ⁹⁰A. Stan, N. E. Dahlen, and R. van Leeuwen, "Fully self-consistent gw calculations for atoms and molecules," *Europhys. Lett.* **76**, 298–304 (2006).
- ⁹¹C. Rostgaard, K. W. Jacobsen, and K. S. Thygesen, "Fully self-consistent gw calculations for molecules," *Phys. Rev. B* **81**, 085103 (2010).
- ⁹²X. Blase, C. Attaccalite, and V. Olevano, "First-principles \$\mathit{mathit{GW}}\$ calculations for fullerenes, porphyrins, phthalocyanine, and other molecules of interest for organic photovoltaic applications," *Phys. Rev. B* **83**, 115103 (2011).
- ⁹³C. Faber, C. Attaccalite, V. Olevano, E. Runge, and X. Blase, "First-principles GW calculations for DNA and RNA nucleobases," *Phys. Rev. B* **83**, 115123 (2011).

- ⁹⁴S.-H. Ke, "All-electron *gw* methods implemented in molecular orbital space: Ionization energy and electron affinity of conjugated molecules," *Phys. Rev. B* **84**, 205415 (2011).
- ⁹⁵F. Bruneval, "Ionization energy of atoms obtained from *gw* self-energy or from random phase approximation total energies," *J. Chem. Phys.* **136**, 194107 (2012).
- ⁹⁶F. Bruneval and M. A. L. Marques, "Benchmarking the Starting Points of the GW Approximation for Molecules," *J. Chem. Theory Comput.* **9**, 324–329 (2013).
- ⁹⁷D. Golze, M. Dvorak, and P. Rinke, "The *gw* compendium: A practical guide to theoretical photoemission spectroscopy," *Front. Chem.* **7**, 377 (2019).
- ⁹⁸A. Marie, A. Ammar, and P.-F. Loos, "The *GW* approximation: A quantum chemistry perspective," in *Advances in Quantum Chemistry*, Novel Treatments of Strong Correlations, Vol. 90 (2024) pp. 157–184.
- ⁹⁹X. Blase, I. Duchemin, and D. Jacquemin, "The bethe–salpeter equation in chemistry: relations with td-dft, applications and challenges," *Chem. Soc. Rev.* **47**, 1022–1043 (2018).
- ¹⁰⁰X. Blase, I. Duchemin, D. Jacquemin, and P.-F. Loos, "The bethe–salpeter equation formalism: From physics to chemistry," *J. Phys. Chem. Lett.* **11**, 7371–7382 (2020).
- ¹⁰¹J. D. Watts and R. J. Bartlett, "The inclusion of connected triple excitations in the equation-of-motion coupled-cluster method," *J. Chem. Phys.* **101**, 3073–3078 (1994).
- ¹⁰²M. Kamiya and S. Hirata, "Higher-order equation-of-motion coupled-cluster methods for ionization processes," *J. Chem. Phys.* **125**, 074111 (2006).
- ¹⁰³J. R. Gour and P. Piecuch, "Efficient formulation and computer implementation of the active-space electron-attached and ionized equation-of-motion coupled-cluster methods," *J. Chem. Phys.* **125**, 234107 (2006).
- ¹⁰⁴M. F. Lange and T. C. Berkelbach, "On the Relation between Equation-of-Motion Coupled-Cluster Theory and the *GW* Approximation," *J. Chem. Theory Comput.* **14**, 4224–4236 (2018).
- ¹⁰⁵G. E. Scuseria, A. C. Scheiner, T. J. Lee, J. E. Rice, and H. F. Schaefer, "The closed-shell coupled cluster single and double excitation (CCSD) model for the description of electron correlation. A comparison with configuration interaction (CISD) results," *J. Chem. Phys.* **86**, 2881–2890 (1987).
- ¹⁰⁶J. F. Stanton, "Many-body methods for excited state potential energy surfaces. I. General theory of energy gradients for the equation-of-motion coupled-cluster method," *J. Chem. Phys.* **99**, 8840–8847 (1993).
- ¹⁰⁷J. Noga and R. J. Bartlett, "The full ccisd model for molecular electronic structure," *J. Chem. Phys.* **86**, 7041–7050 (1987).
- ¹⁰⁸G. E. Scuseria and H. F. Schaefer, "A new implementation of the full CCSDT model for molecular electronic structure," *Chem. Phys. Lett.* **152**, 382–386 (1988).
- ¹⁰⁹K. Kowalski and P. Piecuch, "The active-space equation-of-motion coupled-cluster methods for excited electronic states: Full EOMCCSDt," *J. Chem. Phys.* **115**, 643–651 (2001).
- ¹¹⁰K. Kowalski and P. Piecuch, "Excited-state potential energy curves of CH⁺: A comparison of the EOMCCSDt and full EOMCCSDT results," *Chem. Phys. Lett.* **347**, 237–246 (2001).
- ¹¹¹S. A. Kucharski, M. Włoch, M. Musiał, and R. J. Bartlett, "Coupled-cluster theory for excited electronic states: The full equation-of-motion coupled-cluster single, double, and triple excitation method," *J. Chem. Phys.* **115**, 8263–8266 (2001).
- ¹¹²G. E. Scuseria, T. M. Henderson, and D. C. Sorenson, "The ground state correlation energy of the random phase approximation from a ring coupled cluster doubles approach," *J. Chem. Phys.* **129**, 231101 (2008).
- ¹¹³G. E. Scuseria, T. M. Henderson, and I. W. Bulik, "Particle-particle and quasiparticle random phase approximations: Connections to coupled cluster theory," *J. Chem. Phys.* **139**, 104113 (2013).
- ¹¹⁴D. L. Freeman, "Coupled-cluster expansion applied to the electron gas: Inclusion of ring and exchange effects," *Phys. Rev. B* **15**, 5512–5521 (1977).
- ¹¹⁵G. Jansen, R.-F. Liu, and J. G. Ángyán, "On the equivalence of ring-coupled cluster and adiabatic connection fluctuation-dissipation theorem random phase approximation correlation energy expressions," *J. Chem. Phys.* **133**, 154106 (2010).
- ¹¹⁶D. Peng, S. N. Steinmann, H. van Aggelen, and W. Yang, "Equivalence of particle-particle random phase approximation correlation energy and ladder-coupled-cluster doubles," *J. Chem. Phys.* **139**, 104112 (2013).
- ¹¹⁷T. C. Berkelbach, "Communication: Random-phase approximation excitation energies from approximate equation-of-motion coupled-cluster doubles," *J. Chem. Phys.* **149**, 041103 (2018).
- ¹¹⁸V. Rishi, A. Perera, and R. J. Bartlett, "A route to improving rpa excitation energies through its connection to equation-of-motion coupled cluster theory," *J. Chem. Phys.* **153**, 234101 (2020).
- ¹¹⁹R. Quintero-Monsebaiz, E. Monino, A. Marie, and P.-F. Loos, "Connections between many-body perturbation and coupled-cluster theories," *J. Chem. Phys.* **157**, 231102 (2022).
- ¹²⁰C. J. N. Coveney and D. P. Tew, "Diagrammatic theory of the irreducible coupled-cluster self-energy," *Phys. Rev. B* **112**, 045104 (2025).
- ¹²¹C. J. N. Coveney, "Uncovering relationships between the electronic self-energy and coupled-cluster doubles theory," *J. Phys. Chem. A* **129**, 8689–8698 (2025).
- ¹²²C. J. N. Coveney and D. P. Tew, "Non-hermitian green's function theory with *n*-body interactions: the coupled-cluster similarity transformation," (2025), arXiv:2503.06586 [cond-mat.str-el].
- ¹²³S. J. Bintrim and T. C. Berkelbach, "Full-frequency *gw* without frequency," *J. Chem. Phys.* **154**, 041101 (2021).
- ¹²⁴J. Tölle and G. K.-L. Chan, "Exact relationships between the *gw* approximation and equation-of-motion coupled-cluster theories through the quasi-boson formalism," *J. Chem. Phys.* **158**, 124123 (2023).
- ¹²⁵J. Tölle, "Fully analytic g0w0 nuclear gradients," *J. Phys. Chem. Lett.* **16**, 3672–3678 (2025).
- ¹²⁶J. Tölle, M.-P. Kitsaras, and P.-F. Loos, "Fully analytic nuclear gradients for the bethe–salpeter equation," *J. Phys. Chem. Lett.* **16**, 11134–11143 (2025).
- ¹²⁷M.-P. Kitsaras, J. Tölle, and P.-F. Loos, "Analytic g0w0 gradients based on a double-similarity transformation equation-of-motion coupled-cluster treatment," *J. Chem. Phys.* **164**, 044122 (2026).
- ¹²⁸J. Arponen, "Variational principles and linked-cluster exp s expansions for static and dynamic many-body problems," *Ann. Phys.* **151**, 311–382 (1983).
- ¹²⁹J. Arponen, "The method of stationary cluster amplitudes and the phase transition in the lipkin pseudospin model," *J. Phys. G: Nucl. Phys.* **8**, L129–L134 (1982).
- ¹³⁰J. S. Arponen, R. F. Bishop, and E. Pajanne, "Extended coupled-cluster method. i. generalized coherent bosonization as a mapping of quantum theory into classical hamiltonian mechanics," *Phys. Rev. A* **36**, 2519–2538 (1987).
- ¹³¹J. S. Arponen, R. F. Bishop, and E. Pajanne, "Extended coupled-cluster method. ii. excited states and generalized random-phase approximation," *Phys. Rev. A* **36**, 2539–2549 (1987).
- ¹³²P. Piecuch and R. J. Bartlett, "Eomxcc: A new coupled-cluster method for electronic excited states," (Academic Press, 1999) pp. 295–380.
- ¹³³P.-D. Fan, K. Kowalski, and P. P. *, "Non-iterative corrections to extended coupled-cluster energies employing the generalized method of moments of coupled-cluster equations," *Mol. Phys.* **103**, 2191–2213 (2005).
- ¹³⁴P.-D. Fan and P. Piecuch, "The usefulness of exponential wave function expansions employing one- and two-body cluster operators in electronic structure theory: The extended and generalized coupled-cluster methods," (Academic Press, 2006) pp. 1–57.
- ¹³⁵S. Pal, "Bivariational coupled-cluster approach for the study of static electronic properties," *Phys. Rev. A* **34**, 2682–2686 (1986).
- ¹³⁶S. Pal, "Coupled-cluster response approach: Improved variational strategy," *Phys. Rev. A* **42**, 4385–4387 (1990).
- ¹³⁷K. B. Ghose, P. G. Nair, and S. Pal, "Implementation of a stationary coupled-cluster response method," *Chem. Phys. Lett.* **211**, 15–19 (1993).
- ¹³⁸A. Basu Kumar, N. Vaval, and S. Pal, "An extended coupled-cluster functional for molecular properties: study of an analytical and numerical approach," *Chem. Phys. Lett.* **295**, 189–194 (1998).
- ¹³⁹P. U. Manohar, N. Vaval, and S. Pal, "Extended coupled-cluster approach for magnetizabilities of small molecules," *Chem. Phys. Lett.* **387**, 442–447 (2004).
- ¹⁴⁰R. J. Bartlett and J. Noga, "The expectation value coupled-cluster method and analytical energy derivatives," *Chem. Phys. Lett.* **150**, 29–36 (1988).
- ¹⁴¹R. J. Bartlett, S. A. Kucharski, and J. Noga, "Alternative coupled-cluster ansätze II. The unitary coupled-cluster method," *Chemical Physics Letters* **155**, 133–140 (1989).

- ¹⁴²B. Cooper and P. J. Knowles, "Benchmark studies of variational, unitary and extended coupled cluster methods," *J. Chem. Phys.* **133**, 234102 (2010).
- ¹⁴³F. A. Evangelista, "Alternative single-reference coupled cluster approaches for multireference problems: The simpler, the better," *J. Chem. Phys.* **134**, 224102 (2011).
- ¹⁴⁴T. Van Voorhis and M. Head-Gordon, "The quadratic coupled cluster doubles model," *Chem. Phys. Lett.* **330**, 585–594 (2000).
- ¹⁴⁵E. L. Shirley, "Self-consistent gw and higher-order calculations of electron states in metals," *Phys. Rev. B* **54**, 7758–7764 (1996).
- ¹⁴⁶R. Del Sole, L. Reining, and R. W. Godby, "Gw Γ approximation for electron self-energies in semiconductors and insulators," *Phys. Rev. B* **49**, 8024–8028 (1994).
- ¹⁴⁷A. Schindlmayr and R. W. Godby, "Systematic Vertex Corrections through Iterative Solution of Hedin's Equations Beyond the GW Approximation," *Phys. Rev. Lett.* **80**, 1702–1705 (1998).
- ¹⁴⁸A. J. Morris, M. Stankovski, K. T. Delaney, P. Rinke, P. García-González, and R. W. Godby, "Vertex corrections in localized and extended systems," *Phys. Rev. B* **76**, 155106 (2007).
- ¹⁴⁹M. Shishkin, M. Marsman, and G. Kresse, "Accurate quasiparticle spectra from self-consistent gw calculations with vertex corrections," *Phys. Rev. Lett.* **99**, 246403 (2007).
- ¹⁵⁰P. Romaniello, S. Guyot, and L. Reining, "The self-energy beyond GW: Local and nonlocal vertex corrections," *J. Chem. Phys.* **131**, 154111 (2009).
- ¹⁵¹P. Romaniello, F. Bechstedt, and L. Reining, "Beyond the GW approximation: Combining correlation channels," *Phys. Rev. B* **85**, 155131 (2012).
- ¹⁵²A. Grüneis, G. Kresse, Y. Hinuma, and F. Oba, "Ionization potentials of solids: The importance of vertex corrections," *Phys. Rev. Lett.* **112**, 096401 (2014).
- ¹⁵³L. Hung, F. Bruneval, K. Baishya, and S. Ogut, "Benchmarking the GW Approximation and Bethe-Salpeter Equation for Groups IB and IIB Atoms and Monoxides," *J. Chem. Theory Comput.* **13**, 2135–2146 (2017).
- ¹⁵⁴E. Maggio and G. Kresse, "Gw vertex corrected calculations for molecular systems," *J. Chem. Theory Comput.* **13**, 4765–4778 (2017).
- ¹⁵⁵Y. Wang, P. Rinke, and X. Ren, "Assessing the $G_0W_0\Gamma(1)$ Approach: Beyond G_0W_0 with Hedin's Full Second-Order Self-Energy Contribution," *J. Chem. Theory Comput.* **17**, 5140–5154 (2021).
- ¹⁵⁶C. Mejuto-Zaera and V. c. v. Vlček, "Self-consistency in gw Γ formalism leading to quasiparticle-quasiparticle couplings," *Phys. Rev. B* **106**, 165129 (2022).
- ¹⁵⁷A. Förster and L. Visscher, "Exploring the statically screened G_3W_2 correction to the GW self-energy: Charged excitations and total energies of finite systems," *Phys. Rev. B* **105**, 125121 (2022).
- ¹⁵⁸G. Weng, R. Mallarapu, and V. Vlček, "Embedding vertex corrections in GW self-energy: Theory, implementation, and outlook," *J. Chem. Phys.* **158**, 144105 (2023).
- ¹⁵⁹M. Wen, V. Abraham, G. Harsha, A. Shee, K. B. Whaley, and D. Zgid, "Comparing self-consistent GW and vertex-corrected G_0W_0 ($G_0W_0\Gamma$) accuracy for molecular ionization potentials," *J. Chem. Theory Comput.* **20**, 3109–3120 (2024).
- ¹⁶⁰F. Bruneval and A. Förster, "Fully dynamic G_3W_2 self-energy for finite systems: Formulas and benchmark," *J. Chem. Theory Comput.* **20**, 3218–3230 (2024).
- ¹⁶¹A. Förster and F. Bruneval, "Why does the GW approximation give accurate quasiparticle energies? The cancellation of vertex corrections quantified," *J. Phys. Chem. Lett.* **15**, 12526–12534 (2024).
- ¹⁶²A. Förster, "Beyond quasi-particle self-consistent GW for molecules with vertex corrections," *J. Chem. Theory Comput.* **21**, 1709–1721 (2025).
- ¹⁶³E. Monino and P.-F. Loos, "Unphysical discontinuities, intruder states and regularization in gw methods," *J. Chem. Phys.* **156**, 231101 (2022).
- ¹⁶⁴E. Monino and P.-F. Loos, "Connections and performances of green's function methods for charged and neutral excitations," *J. Chem. Phys.* **159**, 034105 (2023).
- ¹⁶⁵J. Tölle and G. Kin-Lic Chan, "Ab- g_0w_0 : A practical g_0w_0 method without frequency integration based on an auxiliary boson expansion," *J. Chem. Phys.* **160**, 164108 (2024).
- ¹⁶⁶C. J. C. Scott, O. J. Backhouse, and G. H. Booth, "A "moment-conserving" reformulation of gw theory," *J. Chem. Phys.* **158**, 124102 (2023).
- ¹⁶⁷A. Marie and P.-F. Loos, "A Similarity Renormalization Group Approach to Green's Function Methods," *J. Chem. Theory Comput.* **19**, 3943–3957 (2023).
- ¹⁶⁸B. I. Lundqvist, "Characteristic structure in core electron spectra of metals due to the electron-plasmon coupling," *Phys. Kondens. Materie.* **9**, 236–248 (1969).
- ¹⁶⁹D. C. Langreth, "Singularities in the X-Ray Spectra of Metals," *Phys. Rev. B* **1**, 471–477 (1970).
- ¹⁷⁰L. Hedin, "Effects of Recoil on Shake-Up Spectra in Metals," *Phys. Scr.* **21**, 477–480 (1980).
- ¹⁷¹L. Hedin, "On correlation effects in electron spectroscopies and the gw approximation," *J. Phys. Condens. Matter* **11**, R489–R528 (1999).
- ¹⁷²P. Ring and P. Schuck, *The Nuclear Many-Body Problem* (Springer, 2004).
- ¹⁷³T. M. Henderson, I. W. Bulik, T. Stein, and G. E. Scuseria, "Seniority-based coupled cluster theory," *J. Chem. Phys.* **141**, 244104 (2014).
- ¹⁷⁴T. M. Henderson, I. W. Bulik, and G. E. Scuseria, "Pair extended coupled cluster doubles," *J. Chem. Phys.* **142**, 214116 (2015).
- ¹⁷⁵M. D. Prasad, S. Pal, and D. Mukherjee, "Some aspects of self-consistent propagator theories," *Phys. Rev. A* **31**, 1287 (1985).
- ¹⁷⁶B. Datta, D. Mukhopadhyay, and D. Mukherjee, "Consistent propagator theory based on the extended coupled-cluster parametrization of the ground state," *Phys. Rev. A* **47**, 3632 (1993).
- ¹⁷⁷D. Mukherjee and W. Kutzelnigg, "An effective liouvillean formalism for propagators in fock space: Connection with effective hamiltonian approach for energy differences," in *Many-Body Methods in Quantum Chemistry: Proceedings of the Symposium, Tel Aviv University 28–30 August 1988* (Springer, 1989) pp. 257–274.
- ¹⁷⁸Y. Kim and A. I. Krylov, "Two algorithms for excited-state quantum solvers: Theory and application to com-uccsd," *J. Phys. Chem. A* **127**, 6552–6566 (2023).
- ¹⁷⁹J. T. Phillips, L. N. Koulias, S. H. Yuwono, and A. E. D. III, "Comparing perturbative and commutator-rank-based truncation schemes in unitary coupled-cluster theory," *Mol. Phys.* **123**, e2522382 (2025).
- ¹⁸⁰L. Grazioli, M.-P. Kitsaras, and S. Stopkowicz, "Unitary coupled-cluster theory for the treatment of molecules in strong magnetic fields," *J. Chem. Theory Comput.* **21**, 12634 (2025).
- ¹⁸¹W. Chen and A. Pasquarello, "Accurate band gaps of extended systems via efficient vertex corrections in gw," *Phys. Rev. B* **92**, 041115 (2015).
- ¹⁸²X. Ren, N. Marom, F. Caruso, M. Scheffler, and P. Rinke, "Beyond the GW approximation: A second-order screened exchange correction," *Phys. Rev. B* **92**, 081104 (2015).
- ¹⁸³B. Cunningham, M. Grüning, P. Azarhoosh, D. Pashov, and M. Van Schilfgaarde, "Effect of ladder diagrams on optical absorption spectra in a quasiparticle self-consistent gw framework," *Phys. Rev. Mat.* **2**, 034603 (2018).
- ¹⁸⁴V. Vlček, "Stochastic vertex corrections: Linear scaling methods for accurate quasiparticle energies," *J. Chem. Theory Comput.* **15**, 6254–6266 (2019).
- ¹⁸⁵M. Rohlffing, "Approximate spatiotemporal structure of the vertex function $\gamma(1, 2; 3)$ in many-body perturbation theory," *Phys. Rev. B* **108**, 195207 (2023).
- ¹⁸⁶B. Cunningham, M. Grüning, D. Pashov, and M. Van Schilfgaarde, "Qs gw: Quasiparticle self-consistent gw with ladder diagrams in w," *Phys. Rev. B* **108**, 165104 (2023).
- ¹⁸⁷F. Bruneval, A. Förster, and Y. Pavlyukh, "Gw+2sosex self-energy made positive semidefinite," *J. Chem. Theory Comput.* **21**, 10223–10240 (2025).
- ¹⁸⁸F. Bruneval, "Improved density matrices for accurate molecular ionization potentials," *Phys. Rev. B* **99**, 041118 (2019).
- ¹⁸⁹F. Bruneval, "Assessment of the linearized gw density matrix for molecules," *J. Chem. Theory Comput.* **15**, 4069–4078 (2019).
- ¹⁹⁰F. Bruneval, M. Rodriguez-Mayorga, P. Rinke, and M. Dvorak, "Improved one-shot total energies from the linearized gw density matrix," *J. Chem. Theory Comput.* **17**, 2126–2136 (2021).
- ¹⁹¹A. Grüneis, M. Marsman, J. Harl, L. Schimka, and G. Kresse, "Making the random phase approximation to electronic correlation accurate," *J. Chem. Phys.* **131**, 154115 (2009).
- ¹⁹²R. Orlando, P. Romaniello, and P.-F. Loos, "The three channels of many-body perturbation theory: GW, particle–particle, and electron–hole T-matrix self-energies," *J. Chem. Phys.* **159**, 184113 (2023).
- ¹⁹³N. H. Beebe and J. Linderberg, "Simplifications in the generation and transformation of two-electron integrals in molecular calculations," *Int. J. Quantum Chem.* **12**, 683–705 (1977).
- ¹⁹⁴T. B. Pedersen, S. Lehtola, I. Fdez. Galván, and R. Lindh, "The versatility of the cholesky decomposition in electronic structure theory," *WIREs:*

- Comput. Mol. Sci. **14**, e1692 (2024).
- ¹⁹⁵E. G. Hohenstein, R. M. Parrish, and T. J. Martínez, “Tensor hypercontraction density fitting. i. quartic scaling second-and third-order möller-plesset perturbation theory,” *J. Chem. Phys.* **137**, 044103 (2012).
- ¹⁹⁶R. M. Parrish, E. G. Hohenstein, T. J. Martínez, and C. D. Sherrill, “Tensor hypercontraction. ii. least-squares renormalization,” *J. Chem. Phys.* **137**, 224106 (2012).
- ¹⁹⁷Y. Pavlyukh, A.-M. Uimonen, G. Stefanucci, and R. van Leeuwen, “Vertex corrections for positive-definite spectral functions of simple metals,” *Phys. Rev. Lett.* **117**, 206402 (2016).
- ¹⁹⁸W. Kutzelnigg, “How many-body perturbation theory (mbpt) has changed quantum chemistry,” *Int. J. Quantum Chem.* **109**, 3858–3884 (2009).
- ¹⁹⁹Q. Sun, T. C. Berkelbach, N. S. Blunt, G. H. Booth, S. Guo, Z. Li, J. Liu, J. D. McClain, E. R. Sayfutyarova, S. Sharma, S. Wouters, and G. K.-L. Chan, “Pyscf: the python-based simulations of chemistry framework,” *WIREs Comput. Mol. Sci.* **8**, e1340 (2018).
- ²⁰⁰Q. Sun, X. Zhang, S. Banerjee, P. Bao, M. Barbry, N. S. Blunt, N. A. Bogdanov, G. H. Booth, J. Chen, Z.-H. Cui, J. J. Eriksen, Y. Gao, S. Guo, J. Hermann, M. R. Hermes, K. Koh, P. Koval, S. Lehtola, Z. Li, J. Liu, N. Mardirossian, J. D. McClain, M. Motta, B. Mussard, H. Q. Pham, A. Pulkkin, W. Purwanto, P. J. Robinson, E. Ronca, E. R. Sayfutyarova, M. Scheurer, H. F. Schurkus, J. E. T. Smith, C. Sun, S.-N. Sun, S. Upadhyay, L. K. Wagner, X. Wang, A. White, J. D. Whitfield, M. J. Williamson, S. Wouters, J. Yang, J. M. Yu, T. Zhu, T. C. Berkelbach, S. Sharma, A. Y. Sokolov, and G. K.-L. Chan, “Recent developments in the PySCF program package,” *J. Chem. Phys.* **153**, 024109 (2020).
- ²⁰¹A. Marie and P.-F. Loos, “Reference Energies for Valence Ionizations and Satellite Transitions,” *J. Chem. Theory Comput.* **20**, 4751–4777 (2024).
- ²⁰²T. H. Dunning, Jr., “Gaussian basis sets for use in correlated molecular calculations. i. the atoms boron through neon and hydrogen,” *J. Chem. Phys.* **90**, 1007 (1989).
- ²⁰³D. E. Woon and T. H. Dunning, Jr., “Gaussian basis sets for use in correlated molecular calculations. III. The atoms aluminum through argon,” *J. Chem. Phys.* **98**, 1358–1371 (1993).
- ²⁰⁴F. Caruso, P. Rinke, X. Ren, M. Scheffler, and A. Rubio, “Unified description of ground and excited states of finite systems: The self-consistent G W approach,” *Phys. Rev. B* **86**, 081102(R) (2012).
- ²⁰⁵F. Caruso, P. Rinke, X. Ren, A. Rubio, and M. Scheffler, “Self-consistent G W : All-electron implementation with localized basis functions,” *Phys. Rev. B* **88**, 075105 (2013).
- ²⁰⁶F. Caruso, M. Dauth, M. J. van Setten, and P. Rinke, “Benchmark of gw approaches for the gw100 test set,” *J. Chem. Theory Comput.* **12**, 5076 (2016).
- ²⁰⁷E. Maggio and G. Kresse, “Correlation energy for the homogeneous electron gas: Exact bethe-salpeter solution and an approximate evaluation,” *Phys. Rev. B* **93**, 235113 (2016).